Sonoception: Synthetic auditory stimulation modulates inhibitory control, heart-brain interactions, and insular activity

Authors

Daniele Di Lernia[1,8,a], Andrea Zaccaro[2,a], Aleksandra M. Herman[3], Valerio Villani[4], Gianluca Finotti[5], Marcello Costantini[6,10], Francesca Ferri[2,10], Manos Tsakiris[4,7,b], Giuseppe Riva[8,9,b]

Affiliations

[1]Department of Theoretical and Applied Sciences, Faculty of Psychology, eCampus University, Novedrate, Italy
[2]Department of Neuroscience, Imaging and Clinical Science, University G. d'Annunzio, Chieti-Pescara, 66100 Chieti, Italy
[3]Laboratory of Brain Imaging, Nencki Institute of Experimental Biology of the Polish Academy of Sciences, Warsaw, Poland
[4]Lab of Action and Body, Department of Psychology, Royal Holloway, University of London, Egham, United Kingdom
[5]Birkbeck, University of London, School of Psychological Sciences, Malet St, London WC1E 7HX
[6]Department of Psychology, University G. d'Annunzio Chieti-Pescara, 66100 Chieti, Italy.
[7]Centre for the Politics of Feelings, School of Advanced Study, University of London, London, United Kingdom
[8]Applied Technology for Neuro-Psychology Lab, IRCCS Istituto Auxologico Italiano, Milan, Italy
[9]Humane Technology Lab, Università Cattolica del Sacro Cuore, Milan, Italy
[10]Institute for Advanced Biomedical Technologies ITAB, University G. d'Annunzio, Chieti-Pescara, 66100 Chieti, Italy.

[a]These authors contributed equally to this work and share first authorship

[b]These authors contributed equally to this work and share last authorship

Contact information

Correspondence concerning this article should be addressed to Daniele Di Lernia, Department of Theoretical and Applied Sciences, Faculty of Psychology, eCampus University, Novedrate, Italy, daniele.dilernia@uniecampus.it

Abstract

We present a non-invasive stimulation technique called Sonoception that utilizes synthetic auditory frequencies at 6Hz and 2Hz to modulate behavioral, physiological, and neural responses in healthy humans. In three studies, we investigated the effects of Sonoception on emotional processing and inhibitory control, cortical processing of cardiac signals, and brain activation patterns. In Study 1, participants completed a Go/No-go task with faces showing disgusted or neutral expressions to assess the influence of the auditory stimulation on inhibitory control in emotional contexts. The 6Hz stimulation decreased false alarms for neutral faces, whereas the 2Hz stimulation increased false alarms for disgusted faces. This suggested a facilitatory effect of the 6Hz frequency on inhibitory control and a disinhibitory effect of the 2Hz frequency that enhanced impulsive responses. In Study 2, we assessed the heartbeat-evoked potentials as an index of heart-brain interaction and observed increased amplitude following 6Hz stimulation, suggesting enhanced cortical processing of cardiac signals. In Study 3, passive listening fMRI showed that the 6Hz stimulation selectively activated the left insula compared to the 2Hz condition. Taken together, these findings demonstrate that Sonoception exerts distinct effects on behavioral, physiological, and neural functions, supporting the hypothesis that auditory frequency-specific stimulation can modulate cognitive-emotional functions, brain-body interactions and insular activation patterns.

Keywords*:* auditory stimulation, inhibitory control, brain-body interactions, insula, EEG, fMRI, heartbeat-evoked potential, interoception, interoceptive technology

Introduction

Everyday experience is rooted in the continuous interaction between external and internal information. Every sensation, perception, and emotion that enriches our daily life arises from the dynamic interplay between external stimuli, bodily states, and higher-order cognitive processes. In this context, the insular cortex, originally identified as the central hub of interoceptive processing (Craig 2002, Craig 2003), is now recognized as a core element that serves the integration between the external and internal landscapes that constitute our sense of self (Craig 2010, Namkung, Kim et al. 2017). Recently, the insula has been described as "an interface between sensation, emotion and cognition" (Zhang, Deng et al. 2024), mediating high-order cognitive processes such as emotion awareness (Singer, Critchley et al. 2009, Gu, Hof et al. 2013, Seth 2013, Seth and Friston 2016, Frot, Mauguière et al. 2022) and emotion recognition, particularly for emotions such as disgust (Wicker, Keysers et al. 2003, Papagno, Pisoni et al. 2016), inhibitory control mechanisms implicated in impulsivity and salience processing (Ghahremani, Rastogi et al. 2015), as well as multisensory integration of bodily perceptions such as heartbeat, respiration, pain, and others (Gogolla 2017, Hassanpour, Simmons et al. 2018, Salomon, Ronchi et al. 2018, Chouchou, Mauguière et al. 2019, Labrakakis 2023).

Although the left and right insula are often coactive across a broad range of processes, certain specific domains show partial lateralization. Specifically, disgust processing appears to involve the left insula more selectively (Wicker, Keysers et al. 2003, Papagno, Pisoni et al. 2016), while other emotions, such as anger, tend to be less lateralized (Mazzola, Arciero et al. 2016, Seok and Cheong 2019). The insular cortex is also related to control inhibition and impulsivity, and to the processing of conflict and interference (Ghahremani, Rastogi et al. 2015). Evidence from Go/No-go (G/NG) tasks found consistent activation of the insular cortex during failures of behavioral inhibition (Dambacher, Sack et al. 2015), interference processing (Menon, Adleman et al. 2001), and

inhibitory control (Happer, Wagner et al. 2021, Cortese, Vatrano et al. 2022). Interestingly, a meta-analysis of 66 fMRI studies showed that only the left insula was consistently activated across all the inhibitory domains assessed via G/NG tasks (Hung, Gaillard et al. 2018).

The insula is also one of the main sources of the heartbeat-evoked potential (HEP), an event-related potential time-locked to the heartbeat that reflects cortical processing of cardiac signals (Kern, Aertsen et al. 2013, Babo-Rebelo, Wolpert et al. 2016, Babo-Rebelo, Buot et al. 2019). Numerous studies have established a link between the amplitude of the HEP and attention to cardiac sensations, accuracy in perceiving cardiac signals, and emotional arousal (Luft and Bhattacharya 2015, García-Cordero, Esteves et al. 2017, Mai, Wong et al. 2018, Petzschner, Weber et al. 2019). Notably, recent investigations have revealed alterations in HEP amplitude following exposure to sounds associated with disgust (Kato, Takei et al. 2020). This phenomenon was accompanied by heightened insular activity, consistent with prior research that underscores the intricate connection between the perception of disgust and activation of insular cortex (Wicker, Keysers et al. 2003, Wright, He et al. 2004, Vytal and Hamann 2010, Papagno, Pisoni et al. 2016).

In his seminal works, Craig highlighted that the insular cortex was also capable of processing auditory stimuli (Craig 2009, Craig 2010), referring to an experimental study that reported asymmetric and bilateral insular activation in response to different synthetic auditory frequencies (Ackermann, Riecker et al. 2001). In their study, Ackermann, Riecker et al. (2001) identified two separate frequencies that, in addition to other temporal and frontal areas, were selectively processed by either the left or the right insula. Specifically, a 6Hz synthetic sound frequency preferentially activated the left insula, whereas a 2Hz synthetic sound frequency preferentially activated the right one, with a partial overlapping activation of the left insula as well. Their interpretation aligned with the hypothesis that the insula also contributes to spectrotemporal filtering of auditory signals in a lateralized manner, consistent with the “double filtering by

frequency" model (Bamiou, Musiek et al. 2003). According to the theory, in support of language auditory perception, the left insula functions as a high-pass filter, selectively enhancing rapid acoustic transients such as consonants, whereas the right insula serves as a low-pass filter, preferentially processing slower temporal fluctuations such as prosody (Ackermann, Riecker et al. 2001, Ackermann and Riecker 2004). In recent years, accumulating evidence from neuroimaging, lesion studies, and intracranial recordings converges to implicate the insula in processes ranging from low-level acoustic feature encoding (Zhang, Zhou et al. 2019, Berger, Kawasaki et al. 2025, Christison-Lagay, Khalaf et al. 2025) to high-level salience attribution (Blenkmann, Collavini et al. 2019), language perception and comprehension (Remedios, Logothetis et al. 2009, Oh, Duerden et al. 2014, Protas 2018, Nourski, Steinschneider et al. 2022, Zhang, Zhou et al. 2022), and multisensory audio-visual integration (Herdener, Lehmann et al. 2009, Renier, Anurova et al. 2009, Gogolla 2017). Surprisingly, the seminal findings demonstrating lateralized activation of the left and right insula in response to sounds have not been replicated to date, nor have the potential behavioral and physiological correlates of such lateralized stimulation been systematically investigated.

The present work aims at investigating whether non-invasive synthetic sound stimulation can influence processing not only in terms of insula activation, as originally reported by Ackermann, Riecker et al. (2001), but also in terms of measurable shifts at behavioral and cortical levels. We hypothesize that synthetic sound stimulation might elicit asymmetrical effects on different behavioral, physiological, and neural processes preferentially related to insular cortex, from emotional recognition and control inhibition to cortical processing of cardiac signals. We define this methodology as Sonoception (Riva, Serino et al. 2017) and presents the concept of auditory Sonoceptive priming – namely using synthetic auditory stimulation to modulate the processing of subsequent stimuli presented after the stimulation.

We conducted three separate studies aimed at assessing the effects of the auditory stimulation in healthy participants on emotional processing and inhibitory control, cortical processing of cardiac signals, and insular cortex activation. In Study 1, we used an emotional G/NG task involving disgusted and neutral facial expressions to assess the effects of sonoceptive stimulation on emotion discrimination, response inhibition, conflict, and interference processing (Tottenham, Hare et al. 2011). We selected faces expressing disgust as the left insula preferentially processes this emotion (Papagno, Pisoni et al. 2016). In Study 2, we verified the ability of sonoceptive stimulation to alter the processing of cardiac information at the cortical level by assessing HEPs amplitude (Park and Blanke 2019, Coll, Hobson et al. 2021). In Study 3, we sought to replicate the results from Ackermann, Riecker et al. (2001) using passive listening fMRI to confirm that the sonoceptive stimulation activates the insular cortex. Firstly, we expected that the 6Hz auditory stimulation would promote inhibitory control, suppressing inadequate motor response during high-arousal interference contexts, possibly impairing emotion recognition processing for disgusted faces, as suggested by previous literature on left insula direct electrical stimulation (Papagno, Pisoni et al. 2016). Conversely, we predicted that the 2Hz stimulation would have an opposite effect, impairing motor inhibition control and fostering impulsive response for faces expressing disgust. Secondly, we expected an effect of the auditory stimulation on HEPs amplitude, yet we did not formulate specific predictions regarding the lateralization of the two synthetic frequency, as the existing findings on the relationship between the left and right insula and the HEP are inconsistent (Park, Bernasconi et al. 2016, Park, Bernasconi et al. 2018, Babo-Rebelo, Buot et al. 2019). Lastly, we expected to replicate previous fMRI results from Ackermann, Riecker et al. (2001), confirming that the synthetic auditory frequencies can activate the insular cortices in a lateralized manner.

Study 1

Materials and methods

Overview

In Study 1, participants performed an emotional G/NG task with neutral and disgust emotions. The task was repeated three times, at baseline, after the sonoceptive 2Hz stimulation, and after the sonoceptive 6Hz stimulation. The order of the stimulation was counterbalanced, and autonomic (heart rate variability-HRV and galvanic skin response-GSR) data were collected throughout the baseline and the stimulation conditions to control that observed differences in behavioral task among conditions were not explained by changes in physiology.

Participants

Forty-four healthy volunteers with normal or corrected-to-normal vision and no hearing impairments (40 females; mean age = 21.54, SD = 4.87 years old, 40 right-handed) were recruited via the SONA system at Royal Holloway University of London. Inclusion criteria were: no personal/familiar history of neuro-psychiatric, cardiovascular, and/or respiratory disorders; not currently pregnant; no alcohol/drugs taken 24h prior to the experiment or coffee taken 2h prior the experiment. The sample size was estimated based on previous research employing G/NG paradigms (Tottenham, Hare et al. 2011). The research was approved by the University's Ethical Committee at Royal Holloway University of London. Eligible participants were given oral and written explanations about the study procedure. All participants gave written informed consent and received £5 as compensation for their time.

Sonoceptive stimulation

Following (Ackermann, Riecker et al. 2001), a series of isochronous trains of synthetic clicks were created with Audacity® (audacityteam.org). Starting from a single synthetic generated click noise (Fig. 1A and 1B), the original sample was cloned in several train series. Each series was 6s long, each track included 15 trials per frequency in a counter-balanced order. The onset-to-onset intervals between activation and rest epochs randomly varied between 12s and 24s. The auditory stimuli were applied via headphones simultaneously to both ears, volume was then adjusted to a comfortable level and each participant gave oral confirmation of clearly hearing the stimulation. Participants were instructed to passively listen to the acoustic stimuli and to refrain from any motor or cognitive responses such as finger lifting and silent or overt counting. Sonoception audio files are available at OSF material repository (https://osf.io/u5aw3/).

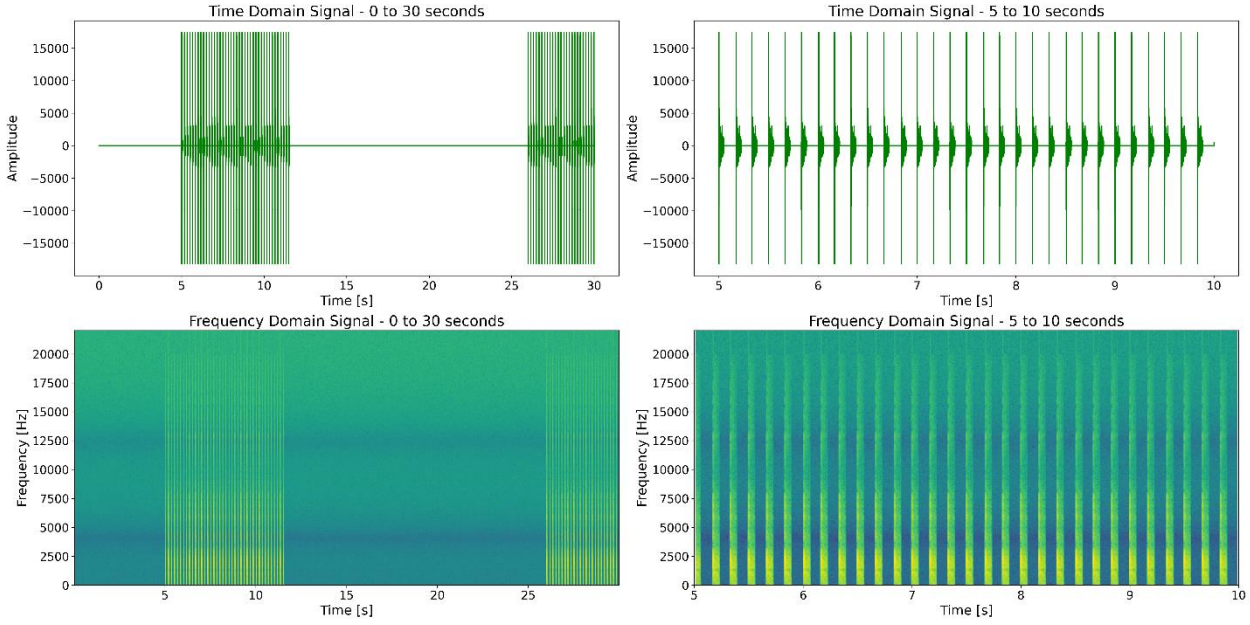

Figure 1A. Visualization of the 6Hz audio signal in the time and frequency domains. (Top left) Time domain signal - First 30 seconds: The plot shows the amplitude of the audio signal over time. (Bottom left)

Frequency domain signal - First 30 seconds: The plot displays the power spectral density of the audio signal across different frequencies over time. (Top right) Time domain signal - 5 to 10 seconds: The plot shows the amplitude of the audio signal in the 5 to 10 seconds segment. (Bottom right) Frequency domain signal - 5 to 10 seconds: The plot displays the power spectral density of the audio signal in the 5 to 10 seconds segment.

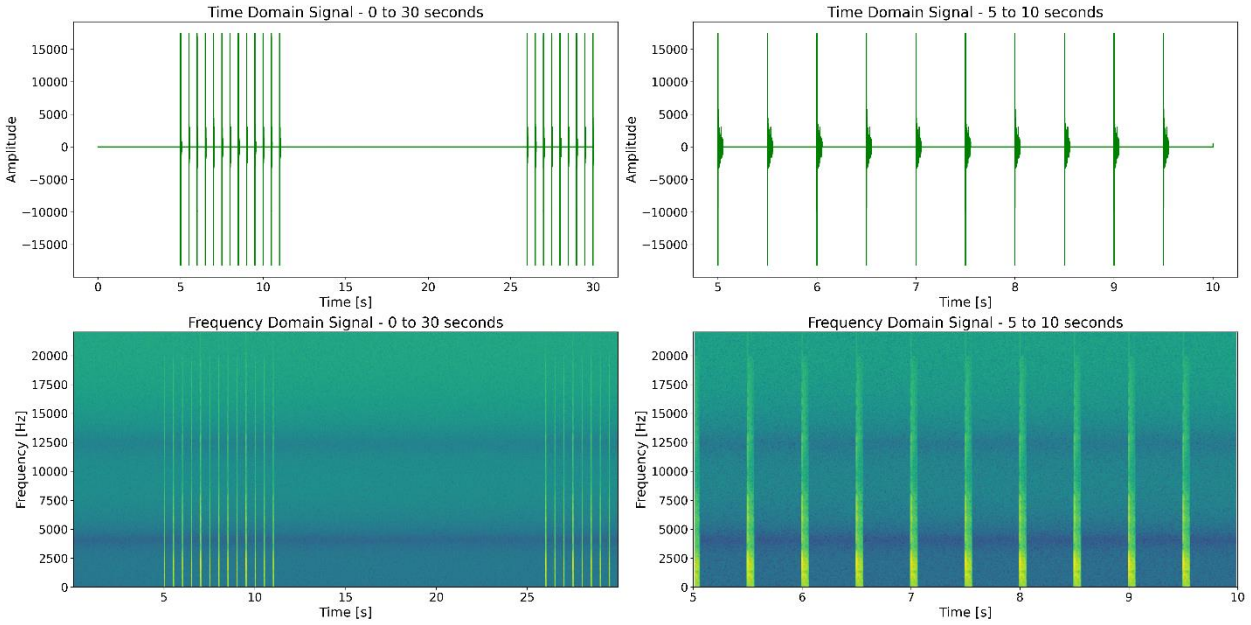

Figure 1B. Visualization of the 2Hz audio signal in the time and frequency domains. (Top left) Time domain signal - First 30 seconds: The plot shows the amplitude of the audio signal over time. (Bottom left) Frequency domain signal - First 30 seconds: The plot displays the power spectral density of the audio signal across different frequencies over time. (Top right) Time domain signal - 5 to 10 seconds: The plot shows the amplitude of the audio signal in the 5 to 10 seconds segment. (Bottom right) Frequency domain signal - 5 to 10 seconds: The plot displays the power spectral density of the audio signal in the 5 to 10 seconds segment.

Procedure

Emotional Go/No-go task

The emotional G/NG task (Tottenham, Hare et al. 2011) is a variation of the standard G/NG task. The task assesses participants' ability to withhold prepotent behavioral responses (cognitive control) in the context of potentially interfering emotional information (emotion regulation). Additionally, the task assesses the ability to discriminate the emotionally relevant stimuli with speed and accuracy (emotion discrimination), which serves both the cognitive control and the emotion regulation processes. For the task, 120 images of neutral and disgusted facial expressions from the FACES database (half males, half neutral) (Ebner et al. 2010) were used. We selected faces expressing disgust due to a cortical asymmetry that indicates how the left insula preferentially processes disgust (Papagno, Pisoni et al. 2016).

Behavioural paradigm

Participants sat comfortably in an armchair, received information regarding the study, and were invited to sign a consent form. Participants were then connected to a 3-lead ECG and 2-lead GSR recorder and invited to rest for 2 minutes before recording the physiological baseline for 5 minutes. After the baseline, participants started the G/NG task. Stimuli were presented on a computer screen. Participants were asked to press a keyboard as they saw a specific emotion indicated by the instructions. The experiment entailed three iterations of the G/NG task: baseline, post 6Hz stimulation, and post 2Hz stimulation. Each iteration of the task consisted of two conditions: in one condition, participants were instructed to respond as quickly as possible with a key-press only to neutral faces (Go stimuli) and ignore disgust faces (No-go stimuli); in the other one, participants had to respond to disgust faces (Go stimuli) and ignore the neutral faces (No-go stimuli). Each condition consisted of 40 trials (70% Go trials, to invoke a prepotent tendency for a Go response)

(Fig. 2). The study always began with the baseline run of the task. Next, participants were invited to wear commercial-grade headphones and to adjust the audio volume to a comfortable level. Participants then underwent auditory stimulation (either 2Hz or 6Hz) for 5 minutes followed by another run of the task. The procedure was repeated for the counterbalanced stimulation. The order of the task conditions (Go neutral and Go disgust) was counterbalanced between runs and participants. The order of the stimulation (2Hz or 6Hz) was also counterbalanced.

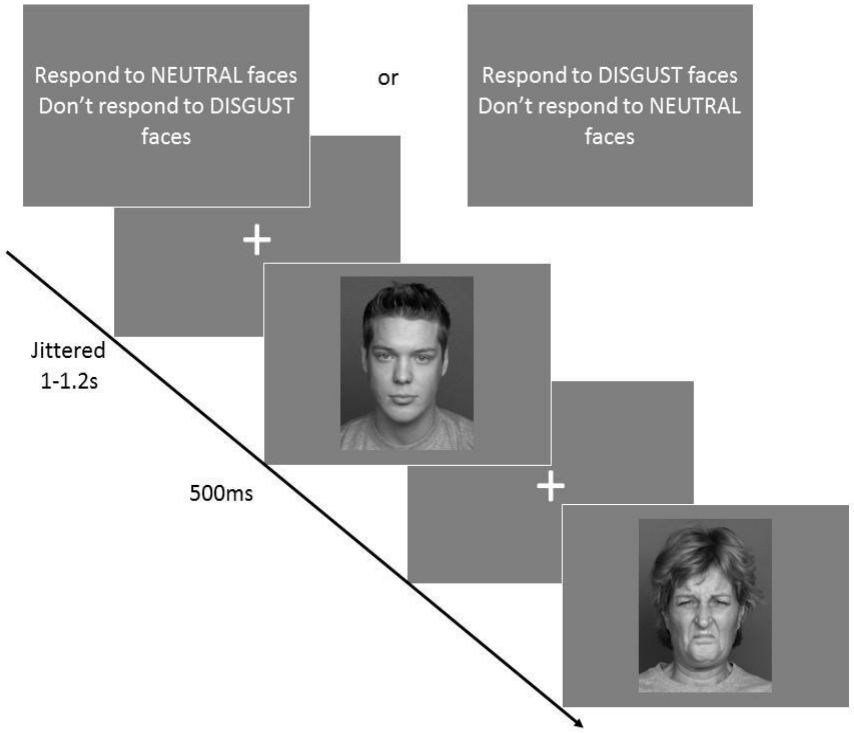

Figure 2. Emotional G/NG task design. The task presented 40 trials per condition for two conditions: disgust and neutral. Each condition included 70% (28) Go trials and 30% (12) No-go trials.

Physiological measures

Cardiac activity (ECG) and GSR were recorded throughout the study. To record participants' ECG, two electrodes were attached under the left and right clavicle and one on the left lower back, within

the ribcage frame. The ECG signal was recorded using a Powerlab 8/35 box (Bio Amp 132, ADInstruments Pty Ltd, Bella Vista, New South Wales, Australia) and LabChart software (v8.1, https://www.adinstruments.com). The sampling rate was 1000 Hz and a hardware band-pass filter between 0.3 and 1000 Hz was applied, as well as a 50 Hz notch filter to reduce electrical noise. Skin conductance Ag/AgCl electrodes (MLT117F, ADInstruments Pty Ltd, Bella Vista, New South Wales, Australia) with 0.5%-NaCl electrode gel were attached to the phalanges of the middle and ring fingers of the participant's non-dominant hand. The signal was recorded using a Powerlab 8/35 box, a GSR Amp unit (22 mV constant voltage at 75Hz) and LabChart software (v8.1) with a recording range of 40 µS and a sampling rate of 1000 Hz. HRV features extraction and analyses were carried out in LabChart. Visual inspection and manual correction were performed to correct unidentified or misidentified peaks. GSR analyses were done using the SCRalyze b2.18 software (http://pspm.sourceforge.net/) according to a convolution model to estimate the area under the curve (AUC), as recommended (Bach, Friston et al. 2010). This approach has been demonstrated to be more effective in predicting autonomic arousal compared to standard analysis techniques. Additionally, it offers the benefits of eliminating the need for subjective assessments and being cost-effective from a computational standpoint (Bach, Friston et al. 2010).

Data analysis

All analyses were performed with R version 4.1.0 (R Core Team 2009). Linear mixed-effects were performed with the *lme4* package (Bates, Mächler et al. 2015). ANOVAs were carried out with the Kenward-Roger approximation and restricted maximum likelihood estimation. All participants were set as having random intercepts. Diagnostic was assured for all models by checking residuals distribution and homoscedasticity with the *performance* package (Lüdecke, Ben-Shachar et al. 2021). *Emmeans* package (Lenth, Singmann et al. 2019) was used to analyze post-hoc with

Bonferroni correction. The response variable is always reported from the predicted values of the linear mixed-effects. The physiological measures for four participants were excluded due to technical difficulties during data collection. We also factored the order of the auditory stimulation into the models, to assess possible interference or carryover effects of the auditory stimulation procedure. The average number of misses and false alarms for each condition, and additional analysis for the order of the stimulation are reported in the Supplementary Materials (Supplementary Tables 1a and 1b).

Go reaction times

Go reaction times (GoRTs) measured in milliseconds were calculated for Go trials only, either for neutral or disgusted faces. GoRTs reflect the speed of information processing and can be used as a proxy for attention.

False alarms

Number of false alarms describe commission errors, namely when a participant fails to withhold their response on the No-go trial. Total false alarm scores were calculated for each emotion condition. Note that for each condition, false alarms and hits are tied to the opposite emotion; for instance, if the Go condition is neutral, the participant must respond to neutral faces and withhold the response for disgusted faces. Pressing the key for disgusted faces will therefore result in a false alarm. False alarms are a measure of impulsive behavior. Specifically, false alarm scores for neutral No-go trials are a proxy of cognitive control – namely a reduced ability to inhibit a prepotent behavioral response in the context of neutral information. Conversely, false alarm rate for disgust No-go trials can be considered an index of emotion regulation – namely a reduced ability to inhibit

a prepotent behavioral response in the context of emotional information (Tottenham, Hare et al. 2011).

Misses

Number of misses quantifies when an individual fails to respond to a designated stimulus and constitutes a crucial indicator of the individual's ability to accurately differentiate the specified emotional expression.

Physiological measures

To evaluate possible effects of the auditory stimulation on the autonomic system that could have interfered with G/NG task performances, we compared a set of cardiac and skin conductance features of interest: heart rate (HR), standard deviation of NN intervals (SDNN), root mean square of the successive differences (RMSSD), HRV total power, high frequency (HF) band power (0.15-0.4 Hz), low frequency (LF) band power (0.04-0.15 Hz), LF/HF ratio, and GSR-AUC. These features were compared across conditions (baseline, post auditory 6Hz stimulation, and post auditory 2Hz stimulation, controlling for the order of stimulation).

Results

Go reaction times

A linear mixed-effects model was fitted using GoRTs as the dependent variable, condition (baseline, post 6Hz, and post 2Hz), emotion (disgust and neutral), and order (2 = 2Hz first and 1 = 6Hz first) as fixed factors, and participant ID as random factor. There was no significant main effect of condition ($p = 0.11$) and no significant interaction between condition and emotion on GoRTs ($p = 0.563$). However, there was a significant main effect of emotion ($F(1, 209.03) = 42.27$,

$p < .001$, partial $\eta^2 = .17$). There was also a significant interaction effect between condition and order ($F(2, 221.14) = 3.47$, $p = .032$, partial $\eta^2 = .03$) and between emotion and order ($F(1, 209.3) = 7.34$, $p = .007$, partial $\eta^2 = .03$). Emotion main effect post-hocs revealed that there was a significant difference in GoRTs between disgust and neutral emotions (Mean disgust = 437 ms, SE = 8.61; Mean neutral = 458 ms, SE = 8.61; $t(209) = -6.502$, $p < .0001$), as disgust was processed faster than neutral (Mean difference = -20.9 ms, SE = 3.22). Additional post-hoc analyses are provided in the Supplementary materials.

False alarms

A linear mixed-effects model was fitted using the false alarms as the dependent variable, condition (baseline, post 6Hz, and post 2Hz), emotion (disgust and neutral) and order (2 = 2Hz first and 1 = 6Hz first) as fixed factors, and participant ID as random factor. The results showed a significant main effect of condition ($F(2, 217.88) = 7.274$, $p = .001$, partial $\eta^2 = .06$), a significant main effect of order ($F(1, 225.32) = 7.391$, $p = .007$, partial $\eta^2 = .03$), and a significant interaction between condition and emotion ($F(2, 209.31) = 4.372$, $p = .014$, partial $\eta^2 = .04$). Post-hoc analyses for the interaction between condition and emotion revealed that for the disgust emotion (i.e., motor inhibition during neutral faces, Fig. 3, left panel), the false alarms in the 6Hz condition (Mean = 0.878, SE = 0.187) were significantly lower than the baseline condition (Mean difference = 0.674, SE = 0.229, $t(215) = 2.94$, $p = .011$). There was no significant difference between the baseline condition (Mean = 1.552, SE = 0.168) and the 2Hz condition ($t(209) = 0.563$, $p = 1$). However, there was a significant difference between the 2Hz (Mean = 1.431, SE = 0.167) and the 6Hz condition (Mean difference = 0.553, SE = 0.23, $t(217) = -2.411$, $p = .050$). For neutral emotion (i.e., motor control inhibition during disgusted faces, Fig. 3, right panel), there was no significant difference between the baseline (Mean = 0.977, SE = 0.168) and the 6Hz condition ($t(215) = -$

334 0.136, p = 1), but there was a significant difference between the baseline and the 2Hz condition
335 (Mean = 1.7, SE = 0.167) (Mean difference = -0.7234, SE = 0.214, t(209) = -3.374, p = .003).
336 There was also a significant difference between the 6Hz (Mean = 1, SE = 0.187) and the 2Hz
337 condition (Mean difference = -0.692, SE = 0.23, t(217) = -3.016, p = .009).

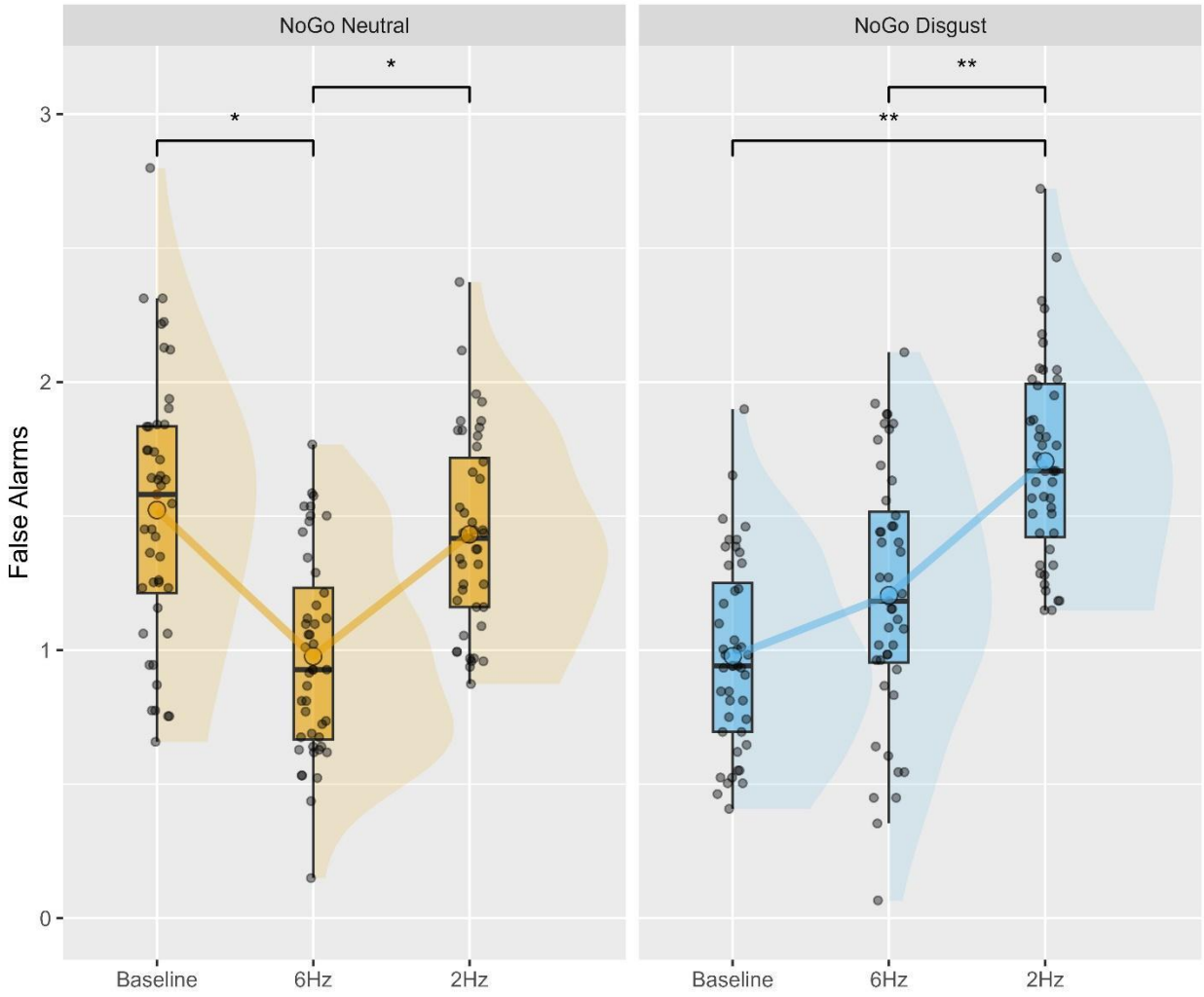

338

339 **Figure 3. False alarms for NoGo Neutral and NoGo Disgust.** Linear mixed-effects model predicting
340 values for comparing baseline, post 6Hz, and post 2Hz sonoceptive stimulation in both Go-disgust and Go-
341 neutral task conditions. In Go-disgust trials (left panel), false alarms are for faces depicting neutral
342 expressions, i.e., NoGo Neutral. In Go-neutral trials (right panel), false alarms are for faces depicting
343 disgusted expressions, i.e., NoGo Disgust. The plot shows the distribution of data using half-eye plots and

boxplots, with individual data points jittered for clarity. Mean values are represented by filled circles. Statistically significant differences between conditions are indicated with asterisks: * denotes $p < .05$ and ** indicates $p < .01$.

Post-hoc analyses for the main effect of condition showed that the difference between 6Hz and baseline and the difference between 2Hz and baseline were not significant. However, the difference between 6Hz and 2Hz was significant ($t(224) = -3.80$, $p = .001$). The plot for the main effect of condition is reported in the Supplementary material (Supplementary Figure 1). Post-hoc analyses for the main effect of order indicated lower false alarm rate when 6Hz was presented first (Order 1, Mean = 1.08, SE = 0.123) than after 2Hz (Order 2, Mean = 1.44, SE = 0.112) ($t(225) = -2.713$, $p = .007$). This result indicated that the 2Hz stimulation resulted in a higher false alarm rate when presented before the 6Hz, suggesting a long-lasting carryover effect of the stimulation.

Misses

A linear mixed-effects model was fitted with the miss rate as the dependent variable, condition (baseline, post 6Hz, and post 2Hz), emotion (disgust and neutral), and order (2 = 2Hz first and 1 = 6Hz first) as fixed factors, and participant ID as random factor. The results showed that the order ($F(1,230.61) = 4.37$, $p = .038$, partial $\eta^2 = .02$) had a significant main effect, while condition, emotion, and all the interaction terms were not significant. Post-hoc analysis for the main effect of order is provided in the Supplementary materials.

Physiological measures

Multiple linear mixed-effects models were fitted using the following dependent variables: SDNN, RMSSD, HR, HF, LF, LF/HF, and GSR-AUC. The fixed factors were condition (baseline, post

6Hz, and post 2Hz) and order (2 = 2Hz first and 1 = 6Hz first), emotion factor was not included because of the trial-based task. The participant ID was used as random factor. Results showed no significant main effects or interactions for SDNN, HF, and LF. An order by condition interaction was significant for RMSSD ($F(2, 77.295) = 3.974$, $p = .023$) and HR ($F(2, 77.029) = 5.294$, $p = .007$). Additionally, a main effect of order was found for LF/HF ($F(2, 40.483) = 7.734$, $p = .008$). Post-hoc analyses are provided in the Supplementary materials. Regarding GSR, the model showed a significant main effect of condition ($F(2, 83.328) = 163.733$, $p < .001$, partial $\eta^2 = .80$). The main effect of order and the interaction between condition and order were not significant. Post-hoc analyses showed that the GSR-AUC during the baseline (Mean = 9.1, SE = 0.362) was significantly higher than both 6Hz (Mean = 3.04, SE = 0.36, $t(83.3) = 15.533$, $p < .0001$) and 2Hz (Mean = 2.91, SE = 0.36, $t(83.3) = 15.867$, $p < .0001$). The difference between 6Hz and 2Hz was not significant.

Interim discussion

The results of Study 1 suggest that sonoceptive stimulation can modulate response inhibition processes in the context of emotionally salient stimuli. Specifically, the 6Hz stimulation enhanced cognitive inhibitory control, as evidenced by a reduced false alarm rate when participants were presented with neutral faces in the Go-disgust condition. This result aligns with existing literature proposing a key role of the left insula in inhibitory control (Hung, Gaillard et al. 2018) and may be interpreted as an attenuation of the salience of stimuli in high-arousal contexts characterized by the interference of emotional stimuli. This would have enhanced the ability to inhibit a prepotent behavioral response in the context of neutral information (Tottenham, Hare et al. 2011). Conversely, the 2Hz stimulation appeared to promote impulsivity, as indicated by a higher false alarm rate when participants were presented with faces expressing disgust, in the Go-neutral condition. This may be interpreted as a failure in inhibitory control (Dambacher, Sack et al. 2015),

potentially due to an enhancement of the immediate arousal response and behavioral relevance of highly emotional stimuli that impaired emotion regulation. This may have led to a reduced ability to inhibit a prepotent behavioral response in the context of emotional information (Tottenham, Hare et al. 2011). The absence of significant effects in both the miss rate and GoRT among conditions suggests that the observed differences are not merely a reflection of attentional mechanisms or diminished accuracy in the discrimination of the emotional faces (Frot, Mauguière et al. 2022). Instead, it might indicate that the two stimulations might modulate the neural pathways associated with emotion regulation and control inhibition differently. The 2Hz stimulation could enhance the perceptual saliency of emotional stimuli (disgust), making participants more likely to fail motor response inhibition. On the other hand, the 6Hz stimulation might promote the opposite mechanism, enhancing inhibitory control by possibly reducing the priming effect of high saliency emotional stimuli aimed at interfering with the discrimination of neutral faces. In this regard, the sonoceptive stimulation seems to play a role in the balance between the salience of primed emotional cues and inhibitory control processes. When focusing on the main effect of the order of sonoceptive stimulation, results indicated that the 2Hz stimulation resulted in an overall higher false alarm rate across conditions when played before the 6Hz, suggesting a long-lasting carryover effect of the 2Hz stimulation that contrasted with the facilitating effect of the 6Hz stimulation in terms of inhibitory control.

On the physiological level, GSR revealed a significant reduction in sympathetic arousal following both the 2Hz and 6Hz stimulations compared to baseline but no differences between the two stimulation conditions. Similarly, several broad HRV indices, including SDNN, as well as HF and LF power, showed no significant effects of the stimulation. This lack of a widespread impact suggests that the sonoceptive stimulation's influence on behavior was not merely a byproduct of a generalized shift in autonomic tone, but rather suggests that the divergent behavioral outcomes,

i.e., the enhancement of inhibitory control and the promotion of impulsivity might be attributable to more specific, higher-order modulation. Lastly, the significant interaction between stimulation condition and presentation order for both RMSSD, a marker of parasympathetic vagal tone, and HR itself, aligns with the carryover effects observed in the behavioral data and the main effect of order on the LF/HF ratio further substantiates this interpretation.

In conclusion, the findings from the G/NG task in Study 1 indicate that sonoceptive stimulation can specifically modulate higher-order functions like inhibitory control, possibly via a central modulation pathway. To further explore the possibility of central processing modulation and given the insula's central role in the processing of cardiac signals, an EEG study was conducted to further investigate the relationship between auditory stimulation and cortical processing of heart-brain interaction, as indexed by the HEP.

Study 2

Materials and methods

Overview

In Study 2, we tested the effect of the sonoceptive stimulation on HEPs, to verify the ability of the stimulation to modulate the cortical processing of cardiac signals. We also collected cardiorespiratory data to control that observed differences in HEP activity among conditions were not explained by changes in cardiorespiratory physiology.

Participants

Twenty right-handed healthy volunteers with normal or corrected-to-normal vision and no hearing impairments (15 females; mean age = 28, SD = 5 years old), recruited at "G. d'Annunzio" University of Chieti-Pescara, Italy, took part in the study. The study sample size was estimated through the G*Power 3.1 software (v3.1.9.7; Faul, Erdfelder et al. (2007)). Considering a paired t-test design (two tailed), we estimated a medium-large effect size of Cohen's d = 0.75, in accord with a recent meta-analysis on HEP modulations (Park and Blanke 2019, Coll, Hobson et al. 2021). We set the significance level to alpha = .05, and the desired power (1 - beta) to .85. The total estimated sample size was 18. Self-reported inclusion criteria were: no personal history of neurological, psychiatric, or somatic disorders and not having taken any drug acting directly or indirectly on the central nervous system in the previous week. All participants gave written informed consent. Participants received no compensation for taking part in the experiment. The study was approved by the Institutional Review Board of Psychology, Department of Psychology (Protocol Number 44_26_07_2021_21016). We excluded 2 participants from the testing of HEPs due to highly noisy EEG (N = 18).

Sonoceptive stimulation

Sonoceptive stimulation was performed as in Study 1.

Procedure

Experimental design and procedure

Participants underwent five experimental conditions: (1) an 8-minute open-eyes resting-state condition, during which participants stared at a fixation cross at the center of a computer screen, while freely mind-wandering (baseline); (2) an 8-minute open-eyes listening condition, during which auditory stimulation was performed at a frequency of 2Hz (stim 2Hz), immediately followed by (3) an 8-minute open-eyes resting-state condition (post 2Hz); (4) an 8-minute open-eyes auditory stimulation at a frequency of 6Hz (stim 6Hz), immediately followed by (5) an 8-minute open-eyes resting-state condition (post 6Hz). The baseline condition was always presented first, while the order of presentation of auditory stimulations (2Hz and 6Hz) was counterbalanced between participants. The sounds presented were at a clearly audible volume, as verbally reported. The auditory stimulation was performed in loop for 8-minute conditions to collect enough HEP epochs for the analysis. The total experimental duration was 40 minutes.

Electrophysiological recordings

EEG signals were acquired with a 64 electrodes BrainAmp EEG acquisition system (BrainCap MR, BrainVision, LLC, Garner, NC, USA), using the midfrontal electrode (FCz) as reference point and the inion electrode (Iz) as the ground. Impedance was kept lower than 10 kΩ for all electrodes. Cardiac signals were recorded with an ECG electrode integrated in the EEG net, placed over the left breast. A second single-lead ECG using three electrodes, two located over the left and right clavicles, and the ground placed on the right costal margin (MP160 BIOPAC Systems, Inc, Goleta,

CA, USA), served as a backup. Respiratory signal was acquired with a piezoelectric respiratory belt positioned around the chest (respiratory transducer TSD201, BIOPAC Systems, Inc, Goleta, CA, USA). All signals were simultaneously recorded throughout the experiment with a sampling rate of 2000 Hz, applying a band-pass filtering from 0.016 to 250 Hz, and a 50 Hz notch filtering.

Electrophysiological data pre-processing

All signals were down-sampled offline to 256 Hz. EEG data were pre-processed with the EEGLAB toolbox (v2021.1; Delorme and Makeig (2004)). According to standard procedures for HEP analysis (Park and Blanke 2019, Coll, Hobson et al. 2021), data were filtered with a Hamming windowed FIR filter from 0.5 Hz to 40 Hz. Datasets were visually inspected for the manual rejection of noisy segments and bad channels. Removed EEG channels (~5%) were interpolated using their neighboring channels (Junghöfer, Elbert et al. 2000, Al, Iliopoulos et al. 2020). Signals were then submitted to an independent component analysis (ICA) for visualizing and removing independent sources of heartbeat, ocular, and muscle artifacts (FastICA algorithm; Hyvarinen (1999). For removing the cardiac field artifact (CFA), we selected the components whose activities followed the time course of the ECG R-peak, as previously reported (Al, Iliopoulos et al. 2020, Al, Iliopoulos et al. 2021, Zaccaro, Perrucci et al. 2022, Zaccaro, della Penna et al. 2024). Artefact-free EEG signals were re-referenced to the average of all channels (Candia-Rivera, Catrambone et al. 2021, Antonacci, Barà et al. 2023, Barà, Zaccaro et al. 2023).

ECG and respiratory signals were high-pass filtered (0.1 Hz) to remove baseline wander. ECG R-peaks were detected in the ECG trace using the Pan-Tompkins algorithm (Pan and Tompkins 1985). Mis-detected peaks (~1%) were automatically corrected using a validated point process model (Citi, Brown et al. 2012). To perform HRV analysis, the RR interval datasets were processed with the Kubios software (v3.4.3; (Tarvainen, Niskanen et al. 2014). From the

tachogram, we extracted a set of HRV features of interest (Zaccaro, Perrucci et al. 2022). Time-domain parameters of interest were HR, SDNN, and RMSSD. Frequency-domain parameters of interest were HRV total power, HF band power, LF band power, and LF/HF ratio. The breathing rate was determined for each experimental condition and participant by dividing the signal in 60 seconds epochs (50% overlap). Each epoch was submitted to a Hanning windowed fast Fourier transform, and the spectral density for each condition was obtained by averaging epochs pertaining to the condition. The breathing rate (Hz) for each condition was determined by the spectrum density peak (Piarulli, Zaccaro et al. 2018, Zaccaro, Piarulli et al. 2022).

Data Analysis

HEP analysis

HEPs were computed using the ERPLAB toolbox (v8.30; ; Lopez-Calderon and Luck (2014)). Peak latencies were extracted and visually inspected with the HEPLAB toolbox (Perakakis 2019). EEG data were epoched around the R-peak (epoch length: -300 to 600 ms after R-peak). Baseline correction was performed between -100 and 0 ms, as previously reported (Zaccaro, Perrucci et al. 2022). All epochs in which the signal exceeded a peak-to-peak threshold of 100 μV (Villena-González, López et al. 2016) were removed (moving window size: 200 ms; step size: 100 ms). To avoid overlap between HEP activity and the following R-peak residual CFA, we also removed epochs where the R-peak was followed by an R-peak by less than 600 ms (Babo-Rebelo, Buot et al. 2019, Zaccaro, Perrucci et al. 2022). Overall, the percentage of rejected epochs was less than 1%. Significant HEP changes across conditions compared to the baseline (post 2Hz vs. baseline and post 6Hz vs. baseline) were assessed with a cluster-based permutation approach (mass univariate ERP toolbox; Groppe et al., 2011a, 2011b), to correct for multiple comparisons in time and space. Based on our previous research research (Zaccaro, Perrucci et al. (2022), we tested HEP

amplitude at each electrode and time point separately in an early (50-350 ms) and a late time window (350-600 ms) after the R-peak (two-tailed, 10,000 permutations). We excluded external electrodes (F7, F8, FT7, FT8, T7, T8, TP7, TP8, P7, P8, PO7, PO8, O1, O2, Oz, TP9, and TP10) that are susceptible to noise contamination and contribute less to HEP modulations analysis (Coll et al., 2021). We focused on HEPs recorded immediately following auditory stimulation (post 2Hz and post 6Hz), rather than during the stimulation itself (stim 2Hz and stim 6Hz), for two main reasons: i) we hypothesized that the effects of auditory stimulation would develop over time and become relatively stable, and thus might not be immediately observable during the stimulation period; and ii) since we aimed to measure HEP as an index of cortical processing of cardiac interoception, we considered that simultaneous auditory (exteroceptive) stimulation might negatively interfere with the processing of cardiac signals. However, we have also performed additional analyses of the auditory stimulation conditions (stim 2Hz and stim 6Hz).

Source analysis

A standard structural T1-weighted MRI template (ICBM152; Fonov et al., 2009) was employed to estimate the neural sources of EEG signals with the BrainStorm toolbox (v3.241016; Tadel et al. 2011). The lead field matrix was calculated using a 3-shell boundary element model provided by the OpenMEEG toolbox (Gramfort et al., 2010; Kybic et al., 2005). Neural sources were then estimated using the minimum norm estimation method with sLORETA normalization (Pascual-Marqui 2002), while constraining current dipole orientations to be normal to the cortical surface. The cortical surface was down-sampled to 15,000 vertices, with each vertex representing a dipole. To statistically analyze differential HEP amplitude responses between conditions, we employed permutation testing (two-tailed, 10,000 randomizations) in the source space using the FieldTrip toolbox, considering significant non-corrected $p < .005$ (Oostenveld et al. 2011).

Linear mixed-effects models

To statistically evaluate the effects of condition order and duration on HEP amplitude, we entered single-trial HEP values into a linear mixed-effects model comprising 25,066 trials, clustered around 18 participants. Single-trial HEP activity was calculated by averaging the voltage of the significant channels and time-window of observed HEP effects. Values lying outside three standard deviations from the mean were labeled as outliers and consequently excluded. Models were implemented using the general analyses for the linear model (GAMLj) module in jamovi (v2.3.21; The jamovi project 2022), with the residual maximum likelihood method. We computed multiple models to predict HEP amplitude, starting with the simplest model and adding factors stepwise. The Akaike information criterion (AIC) was used to identify the best-fitting model. For each parameter in the best-fitting model, we reported the estimated coefficient (b), standard error (SE), t-statistic, and p-value, with degrees of freedom estimated using Satterthwaite's method. Fixed factors included condition (baseline, post 2Hz and post 6Hz) and order (2Hz first and 6Hz first). To assess the role of task duration, we calculated the relative latency as a covariate, defined as the latency (in seconds) of each R-peak in relation to the beginning of each specific condition. In these models, we examined the interactions between condition × order and condition × latency. When a significant interaction was found, post-hoc analyses were conducted separately for each condition and corrected for multiple comparisons using the Tukey method.

Cardiorespiratory control analyses

For assessing the impact of cardiorespiratory physiology on HEP changes among conditions, we compared the set of cardiac and respiratory features of interest (breathing rate, HR, SDNN, RMSSD, HRV, HF, LF, and LF/HF) across conditions with a repeated measures ANOVA. To assess changes in the cardiac signal, we computed the average ECG signal time-locked to the R-

peak, and compared it across conditions (post 2Hz vs. baseline and post 6Hz vs. baseline) with two-tailed paired t-tests within the time window of observed significant HEP differences (Groppe et al., 2011a), corrected with the false discovery rate (FDR) procedure. FDR threshold was set at p = .05. Effect sizes were computed with Cohen's d and partial η^2 indices. Statistical analyses were performed in jamovi (v2.3.21; The jamovi project 2022).

Results

We characterized HEP activity following two sessions of auditory stimulation at specific sound frequencies (post 2Hz and post 6Hz) and compared it with a resting-state condition (baseline) in both early (50-350 ms post-R-peak) and late (350-600 ms post-R-peak) HEP time-windows. First, we performed a cluster-based permutation t-test comparing HEPs during the baseline condition with those after 2Hz auditory stimulation. This analysis revealed no significant differences in any cortical cluster for either the early ($t(17) = -1.97$, $p = .57$, $d = -0.465$) or late time windows ($t(17) = 0.848$, $p = .232$, $d = 0.199$) (Supplementary Figure 2). We then compared baseline HEPs with those obtained after 6Hz auditory stimulation. During a window from 66 to 309 ms post-R-peak (early time-window), HEP negativity was enhanced in the post 6Hz condition over a central-right cluster of electrodes (FCz, Cz, CPz, C4, C2, CP2, CP4, CP6, P2, and P4), with peaks at Cz, CPz, and C2 ($t(17) = -3.743$, $p = .035$, $d = 0.882$) (Fig. 4A,B). This result suggests increased cortical processing of the heartbeat after 6Hz auditory stimulation. Source reconstruction with sLORETA indicated that HEP amplitude was significantly more negative in the post-6Hz condition than in baseline, particularly in postero-central cortical areas primarily involving the sensorimotor network (bilateral post-central, paracentral, and pre-central gyri) ($t(17) = -3.103$, $p < .005$, $d = -0.731$) (Fig. 4C). No significant HEP differences were found between conditions in the late time window ($t(17)$

= 0.821, p = .99, d = 0.194). We did not observe significant HEP amplitude changes when contrasting the post 6Hz with post 2Hz condition in either the early (t(17) = -2.312, p = .965, d = -0.545) or late (t(17) = 0.264, p = 1, d = 0.062) time windows. We also analyzed whether HEPs differed between baseline and each auditory stimulation period (stim 2Hz and stim 6Hz). As expected, we found no significant differences across comparisons (early time window: stim 6Hz vs. baseline (t(17) = -1.91, p = .376, d = -0.45); stim 2Hz vs. baseline (t(17) = -2.288, p = .63, d = -0.539); stim 6Hz vs. stim 2Hz (t(17) = -0.412, p = 1, d = -0.097); late time window: stim 6Hz vs. baseline (t(17) = 0.841, p = 1, d = 0.192); stim 2Hz vs. baseline (t(17) = 1.585, p = .614, d = 0.374); and stim 6Hz vs. stim 2Hz (t(17) = -1.004, p = .351, d = -0.237); see Supplementary Figure 3A,B).

To determine whether changes in HEP activity were associated with peripheral changes in cardiac or respiratory physiology across conditions, we examined participants' cardiorespiratory features (breathing rate, HR, SDNN, RMSSD, HRV, HF, LF, and LF/HF) using repeated-measures ANOVAs. No significant differences emerged across conditions (see Supplementary materials, Supplementary Table 3). To assess changes in cardiac physiology, we conducted two-tailed paired t-tests on the average ECG amplitude at each time-point within the significant HEP window (66-309 ms), followed by FDR correction. No significant differences in ECG amplitude were observed between conditions (baseline vs. post 6Hz: t(19) = 1.94, p = .102, d = 0.435) (Fig. 4D). In sum, these analyses suggest that the observed differences in HEP activity between conditions are not attributable to cardiorespiratory physiological changes, but rather to changes in cardiac interoception at the cortical level. To further assess the role of auditory stimulation duration (i.e., relative latency) and order on HEP amplitude, we performed additional analyses using linear mixed-effects models. The best fitting model was:

$$HEP \sim 1 + condition + order + condition{:}\,order + (1|ID)$$

The model reported a significant effect of the intercept (b = -0.08, SE = 0.037, t = -2.195, p = .043) and of condition (not reported), which was trivial considering that HEPs were averaged over the previously significant cluster. Importantly, the model also showed a significant interaction between order and condition (post 2Hz vs. baseline: b = -0.091, SE = 0.033, t = -2.765, p = .006; post 6Hz vs. baseline: b = -0.07, SE = 0.033, t = -2.125, p = .034). No significant effects were found for relative latency, nor for its interactions with condition. Post-hoc analyses revealed a significant increase in negativity for the post 6Hz vs. baseline (z = 4.578, p < .001) and post 2Hz vs. baseline comparisons (z = 4.332, p < .001), but only when the 6Hz condition was presented first. A trend toward increased HEP negativity was observed for the post 6Hz vs. baseline comparison when the 2Hz condition was presented first. However, this did not survive correction for multiple comparisons (z = 2.12, p = .277). No other post-hoc comparisons were significant (Fig. 4E).

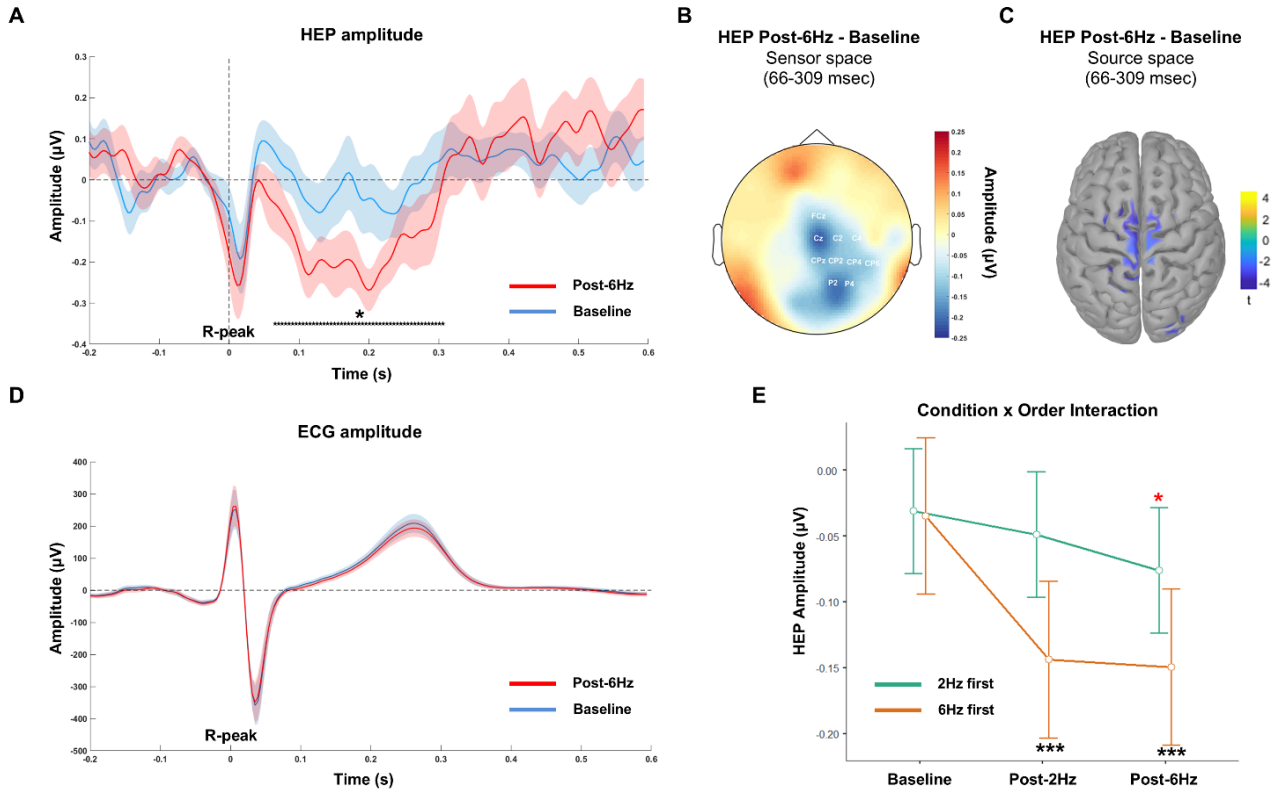

Figure 4. HEP and ECG activity after auditory stimulation. (A) Grand-averaged HEP pooled for significant central-right electrodes (FCz, Cz, CPz, C4, C2, CP2, CP4, CP6, P2, and P4) during the post 6Hz (red) and baseline (blue) conditions. Shaded areas display the standard error of the mean. The black markers show significant differences between conditions (* $p < .05$). (B) The topographical distribution represents HEP differences between the post 6Hz and baseline conditions from 66 to 309 ms after the R-peak. White labels represent significant electrodes. (C) sLORETA source-reconstruction of significant HEP amplitude changes between the post 6Hz and baseline conditions from 66 to 309 ms after the R-peak. (D) Grand-averaged ECG signal during the post 6Hz (red) and baseline (blue) conditions. Shaded areas display the standard error of the mean. (E) Linear mixed-effects model showing the significant condition x order interaction and post-hoc analyses. Error bars represent the standard error of the mean. Red asterisk represents post-hoc analysis against the baseline that did not survive Tukey correction. The three asterisks represent post-hoc analysis against the baseline with a corrected p-value < .001.

Interim discussion

HEP analysis results indicate that 6Hz auditory stimulation can effectively modulate and enhance cortical processing of heartbeat signals, leading to increased HEP negative amplitude over central-right cortices. Control analyses confirmed that differences in HEP activity between conditions cannot be attributed to shifts in cardiorespiratory physiology, but they appear to be linked to cortical processing of cardiac interoceptive signals. This suggests that 6Hz sonoceptive stimulation may enhance heart-brain interactions. Conversely, auditory stimulation at 2Hz did not induce significant increases in HEP negativity. As expected, no significant effect was observed when comparing the auditory stimulation phases (stim 6Hz and stim 2Hz) with the baseline, suggesting that the effects of the stimulation emerge gradually over time. Notably, single-trial mixed-effects model analysis revealed that, as in Study 1, the order of presentation of the auditory stimulations strongly influenced differences in HEP amplitude among post 2Hz, post 6Hz, and baseline conditions. The

mixed-effects model showed that 2Hz auditory stimulation not only fails to increase HEP negativity but also inhibits the effects of subsequent 6Hz auditory stimulation, in a similar manner as the order effect reported in Study 1. In contrast, 6Hz stimulation is robust enough to sustain high HEP negativity even after subsequent 2Hz stimulation, with 2Hz stimulation being associated to higher HEP negativity compared to baseline only when following 6Hz stimulation. This suggests a sustained carryover effect of both stimulations (facilitatory in the case of 6Hz and suppressive for 2Hz) on cardiac interoception. It is noteworthy that the insular cortex has been previously implicated in HEP generation (Canales-Johnson, Silva et al. 2015, Babo-Rebelo, Wolpert et al. 2016, Babo-Rebelo, Buot et al. 2019, Park and Blanke 2019). Given the association of 6Hz auditory stimulation with left insular activation (Ackermann, Riecker et al. 2001), our findings suggest that synthetic auditory stimulation with 6Hz sounds may amplify HEP activity via left insular engagement. This interpretation is partially supported by intracranial EEG evidence in the literature: electrodes implanted in the left insular cortex demonstrated differential HEP modulation between two experimental conditions in a full-body illusion paradigm, where the synchronous stroking condition elicited greater HEP modulation in the left insula compared to the asynchronous condition (Park, Bernasconi et al. 2018). However, literature on the contributions of the left versus right insula to the HEP remains inconsistent. In this regard, the lack of significant HEP response to the 2Hz auditory stimulation may suggest that cortical processing of cardiac information under conditions of low arousal (i.e., passive listening) could be more closely associated with left insular processing. Due to the spatial limitations inherent in EEG, an additional fMRI study was conducted to validate the direct relationship auditory stimulation and insular activity.

Study 3

Materials and methods

Overview

In Study 3, to verify that the sonoceptive stimulation was able to modulate insular activation, participants underwent passive listening fMRI scans. The scans were performed with three runs; baseline (resting-state), sonoceptive 2Hz stimulation, and sonoceptive 6Hz stimulation. The baseline condition was always performed first, while the order of presentation of the auditory stimulation conditions was counterbalanced across participants.

Participants

Thirty right-handed healthy volunteers with normal or corrected-to-normal vision and no hearing impairments (25 females; mean age = 21.9, SD = 3.52 years old) were recruited for the study. Participants had no history of brain injury and showed no MRI contraindications to participate. At the time of testing, none of the participants were taking any medication for neurological or psychological disorders. All participants provided written informed consent in line with the Local Ethics Committee Regulations and MRI Safety Procedures. This research was approved by the University's Ethical Committee at Royal Holloway University of London. Eligible participants were given oral and written explanations about the study procedure. All participants gave written informed consent and received £25 as compensation for their time. The sample size was estimated based on previous research utilizing within-subject design in fMRI. Due to technical issues, one participant was excluded from the analysis entirely and one participant had one invalid run of audio-rest (final sample N = 28).

Sonoceptive stimulation

Sonoceptive stimulation was performed as in Studies 1 and 2.

Procedure

In the MRI scanner, a 6-min resting-state scan (run 1) took place first, during which participants were instructed to rest with their eyes open (without thinking of anything in particular) and not to fall asleep. During the resting-state scan, a white fixation cross was presented in the center of a homogenous gray background. Subsequently, a structural scan was obtained. Next, participants completed two rounds of scans (6 minutes each) while passively listening to sounds (runs 2 and 3; auditory stimulation at 6Hz and 2Hz, in counterbalanced order). Auditory stimuli were applied via headphones simultaneously to both ears and were well discernible at a comfortable loudness level against the background of scanner noise, as confirmed by each participant. Each auditory stimulation run comprised 15 click trains of sounds. Participants were instructed to passively listen to the acoustic stimuli with their eyes open and fixed on the fixation cross and to strictly refrain from any motor or cognitive responses. The onset-to-onset intervals between the click trains varied randomly between 12 and 24 s (jittered interspersed gaps) (Ackermann et al., 2001). The single click trains lasted for approximately 6s. The total time spent in the scanner by each participant did not exceed 60 min.

Data collection

MRI acquisition was performed on a Siemens Magnetom TrioTim syngo MR B17 3-Tesla scanner (Siemens AG, Munich, Germany). Structural volumes were obtained using the high-resolution three-dimensional magnetization prepared rapid acquisition gradient echo sequence (TR = 2.3 s, TE = 2.96 ms, TI = 0.9 s, FA = 11°, 192 sagittal slices per slab, 1 x 1 x 1 mm, FoV = 256 mm,

GRAPPA acceleration factor = 2). Whole-brain multiband gradient echo echo-planar imaging (EPI) sensitive to blood oxygenation–level dependent signal was used to collect fMRI data (multiband acceleration factor = 2, TR = 2000 ms, TE = 30.6 ms, FA = 78°, 50 slices, FoV = 192 mm, voxel size = 2 x 2 x 2 mm). A fieldmap was also acquired using the same resolution and slice locations as multiband images, to allow for offline correction of field inhomogeneities (TR = 525 ms, TE = 5.19/7.65 ms, FA = 60◦, 1:43 min).

fMRI data preprocessing

Imaging analysis was performed using FEAT (FMRI expert analysis tool) version 6.00, a part of FMRIB software library (FSLv6.0, (Jenkinson, Beckmann, Behrens, Woolrich, & Smith, 2012)). Pre-processing steps included skull stripping of structural images with brain extraction tool (BET), removal of the first five functional volumes to allow for signal equilibration, head movement correction by volume-realignment to the middle volume using MCFLIRT, global 4D mean intensity normalization, spatial smoothing (6 mm full-width half-maximum) and noise signals removal, temporal high-pass filtering (Gaussian-weighted least-squares straight line fitting, with sigma = 45.0 s), and fieldmap-based distortion correction. FMRI datasets were co-registered to the participant's structural image using FSL FLIRT (Jenkinson, Bannister, Brady, & Smith, 2002; Jenkinson & Smith, 2001) and subsequently transformed to MNI152 standard space using nonlinear registration through FSL FNIRT (Andersson, Jenkinson, & Smith, 2010). Noise signals were identified individually and removed using ICA-AROMA toolbox (Pruim et al., 2015). ICA-AROMA incorporates probabilistic ICA on the partly pre-processed single-subject fMRI data (following spatial smoothing and normalization but before high-pass filtering), identifies independent components representing motion artefacts and removes them from the fMRI time-series using linear regression. Participants' motion was minimal and did not exceed 2 mm (1 voxel).

Auditory stimulation data analysis

Time-series statistical analysis was carried out using FILM with local autocorrelation correction (Woolrich, Ripley, Brady, & Smith, 2001). In the first-level modelling, waveforms representing onsets and durations of each auditory train were convolved with a double-gamma hemodynamic response function and a high pass filter was applied to remove low-frequency artefacts. There were two different analyses: (1) simple main effect of each auditory stimulation condition and (2) a difference between conditions (6Hz vs. 2Hz). For the main effects analysis, the one-sample t-test was performed to identify activations evoked by sounds (vs. implicit baseline). To identify brain regions differentially recruited between 6Hz and 2Hz auditory stimulation conditions, a second-level (group level) whole brain voxel-wise GLM was conducted across participants. As we had a strong hypothesis regarding between-auditory stimulation differences within the insula, we conducted a separate region of interest (ROI) analysis, were we used bilateral insula mask as defined in the Harvard-Oxford cortical probabilistic atlas (Desikan et al., 2006; Frazier et al., 2005; Makris et al., 2006) thresholded at 95%. The within-subject analysis was carried out using the FMRIB local analysis of mixed effects (FLAME; Woolrich, Behrens, Beckmann, Jenkinson, & Smith, 2004)). Z (Gaussianised T/F) statistic images were thresholded non-parametrically using clusters determined by $Z > 3.1$ and a (corrected) cluster significance threshold of $p = .05$ across the entire brain (Worsley, 2001). The order of auditory stimulation condition (mean centered) was added into a group-level analysis as a covariate to control for potential order-effects.

Results

MRI auditory stimulation

For the main effect of the auditory stimulation vs. baseline, both frequencies (6Hz and 2Hz), evoked bilateral (posterior) insular activations, alongside robust activations in temporal regions

(bilateral planum temporale, primary and secondary auditory cortices, middle and superior temporal gyri), frontal areas (bilateral inferior frontal gyri, frontal pole, frontal operculum), and cerebellar cortices. The 6Hz auditory stimulation also evoked activations within subcortical areas (caudate, putamen, pallidum), while the 2Hz stimulation also activated the right precentral gyrus and brain stem (Table 1, Fig. 5A,B).These results largely replicate previous findings showing that passive listening to click trains (2Hz and 6Hz) elicits hemodynamic activation in several structures outside the central-auditory pathways including the insular cortices (Ackermann, Riecker et al. 2001). The contrast between auditory stimulation conditions (6Hz vs. 2Hz) revealed that the 6Hz frequency evoked greater activation in the bilateral Herschl's gyrus (encompassing primary and secondary somatosensory cortices). However, the changes did not extend into insular cortex (Table 1, Fig. 5C). Subsequent analysis using the bilateral insula as a ROI revealed a greater activation in a small cluster within the left (posterior) insula during the 6Hz compared to the 2Hz auditory stimulation condition (Table 1, Fig. 5D). There were no suprathreshold differences for the reversed contrast.

Table 1. Results of the auditory stimulation analysis presenting the coordinates of clusters peaks. Coordinates are presented in MNI space.

Cluster Size (Voxels)	P	Z-MAX	Z-MAX X	Z-MAX Y	Z-MAX Z	Side	Peak Region
6Hz > baseline (whole brain)							
7870	< .001	6.61	44	-20	2	Right	Planum Temporale
4152	< .001	6.26	-38	-30	10	Left	Planum Temporale
1962	< .001	4.99	-12	-76	-46	Left	Cerebellum
516	< .001	4.05	12	16	4	Right	Caudate
455	< .001	4.37	-18	8	0	Left	Putamen
352	< .001	4.06	-6	34	44	Left	Superior Frontal Gyrus
164	.026	4.14	-40	22	4	Left	Frontal Operculum Cortex
2Hz > baseline (whole brain)							
4640	< .001	6.33	56	-30	10	Right	Planum Temporale
4164	< .001	5.81	-60	-36	12	Left	Superior Temporal Gyrus
938	< .001	5.19	48	22	18	Right	Inferior Frontal Gyrus
690	< .001	5.27	-28	-66	-54	Left	Cerebellum
249	.003	4.96	30	-60	-46	Right	Cerebellum
165	.026	4.48	58	0	50	Right	Precentral Gyrus
159	.030	4.35	10	-28	-6	Right	Brain-Stem
6Hz > 2Hz (whole brain)							
318	< .001	4.86	-34	-28	10	Left	**Planum Temporale**
173	.013	4.82	46	-20	4	Right	Heschl's Gyrus
6Hz > 2Hz (ROI analysis: bilateral insular cortex)							
38	.022	4.61	-32	-26	12	Left	Insular Cortex

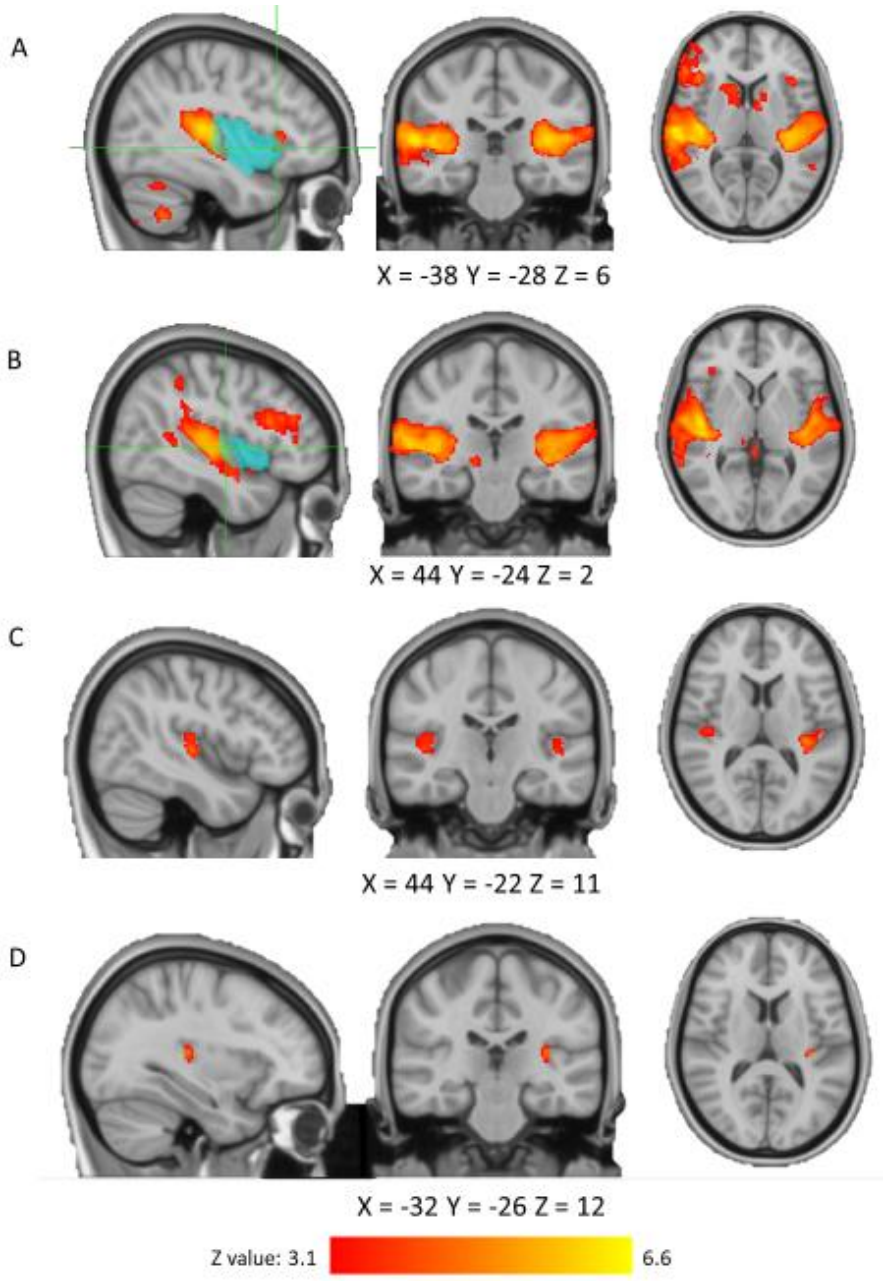

778

779 **Figure 5. Auditory stimulation results.** (A) 6Hz > baseline, (B) 2Hz > baseline, (C) 6Hz > 2Hz (whole
780 brain analysis), (D) 6Hz > 2Hz (ROI analysis). The blue areas in panel A and B depict bilateral insular
781 cortex used in the ROI analysis. Images are presented in the radiological convention: the right side of the
782 brain is depicted in the left side of the image with coordinates in the MNI space.

783

General discussion

In the present study, we tested a non-invasive technique called Sonoception that utilizes synthetic auditory stimulation to modulate behavioral, physiological, and neural responses in healthy participants.

Following preliminary fMRI evidence from of Ackermann, Riecker et al. (2001), we designed two sequencies of artificial train click noises, at prespecified frequencies. These auditory stimulations were previously shown to be able to activate the insular cortex asymmetrically, where a 6Hz synthetic audio stimulation was able to preferentially active the left insula, while a 2Hz synthetic audio stimulation was able to preferentially activate the right insula. We therefore sought to understand if this synthetic auditory stimulation could also modulate various levels of human processing related in literature to the insula activity such as emotion discrimination, inhibitory control, impulsivity, and cardiac heart-brain interaction. Specifically, we expected 6Hz stimulation to enhance inhibitory control of emotionally salient stimuli, and 2Hz to impair motor inhibition and increase impulsivity. Additionally, we explored whether auditory stimulation modulated cortical processing of heart-brain interactions, as indexed by HEP amplitude, though no frequency-specific predictions were made due to inconsistent findings on insular lateralization in cardiac interoception. Lastly, we sought to replicate previous fMRI results from Ackermann, Riecker et al. (2001) demonstrating frequency-specific insular activations.

Study 1 confirmed that Sonoception modulates inhibitory control in emotionally salient contexts. The 6Hz stimulation enhanced response inhibition, reflected by reduced false alarms to neutral faces. Conversely, 2Hz stimulation increased false alarms to disgusted faces. These results align with the literature supporting a dominant role of the left insula in inhibitory control at cognitive, motor, and emotional level (Hung, Gaillard et al. 2018), and it is suggestive that the 6Hz

auditory stimulation was able to diminish the salience in contexts characterized by the interference of high-arousal emotional stimuli. Conversely, the 2Hz stimulation, was able to inhibit a prepotent behavioral response in the context of emotional information (Tottenham, Hare et al. 2011), enhancing impulsive responses. This finding, on the other hand, might be interpreted as a failure of inhibitory control (Dambacher, Sack et al. 2015) due to an enhancement of the immediate arousal value and behavioral relevance of highly emotional stimuli. Interestingly, the absence of significant differences in both the missing number and Go response times suggests that the observed effects did not reflect changes in attentional or emotional discrimination processes (Frot, Mauguière et al. 2022). Moreover, the results on physiological measures indicated that the observed effects could not be attributed to increased autonomic or physiological arousal that might have confounded inhibitory control responses. Notably, despite counterbalancing, we observed a robust carryover effect: 2Hz auditory stimulation preceding 6Hz led to an overall increase in false alarms, indicating a disruptive effect on inhibitory control. This suggests that 2Hz not only elicits impulsivity but may interfere with the facilitatory effects of subsequent 6Hz stimulation.

Study 2 extended these findings to heart-brain dynamics. The 6Hz stimulation enhanced HEP negativity over central-right electrodes immediately post-stimulation, independently of changes in cardiorespiratory physiology, suggesting that passive exposure to 6Hz sound stimulation has the potential to enhance the cortical processing of cardiac signals. In contrast, 2Hz stimulation not only failed to increase HEP amplitude when presented first but also showed a suppressive carryover effect to subsequent 6Hz stimulation. These results mirror the behavioural findings from Study 1, confirming the effects of stimulation frequency on heart-brain interaction. Given the established link between insular activity and HEP generation (Canales-Johnson, Silva et al. 2015, Babo-Rebelo, Wolpert et al. 2016, Babo-Rebelo, Buot et al. 2019) and the association of

6Hz stimulation with left insular activation (Ackermann, Riecker et al. 2001) we propose that the modulation of HEP amplitude is likely mediated by left insular engagement. However, the precise lateralization of insular contributions to cardiac cortical processing remains to be determined.

Study 3 partially replicated the fMRI findings of Ackermann, Riecker et al. (2001). While our paradigm did not employ a parametric design, passive listening to 2Hz and 6Hz click trains elicited hemodynamic responses in both central auditory pathways and the insular cortices. ROI analyses showed significantly greater activation in the left posterior insula during 6Hz relative to 2Hz stimulation, corroborating the behavioural and HEP findings. On the contrary, we did not observe greater right insular activation relative to the left in response to 2Hz stimulation, casting doubt on the efficacy of 2Hz as a right-lateralized insular modulator.

Taken together, these findings add to accumulating evidence positioning the insular cortex as a key hub for auditory perception. The posterior insula is known to be involved in early auditory processing, with activation patterns resembling those of primary auditory areas (Berger, Kawasaki et al. 2025, Christison-Lagay, Khalaf et al. 2025), likely via direct projections from the medial geniculate body and auditory cortices (Mesulam and Mufson 1982, Augustine 1996, Cauda, D'agata et al. 2011, Takemoto, Hasegawa et al. 2014). Nonetheless and more crucially, our findings demonstrate that Sonoception can not only activate the insula but also modulate higher-order functions that related in the literature to this specific area. The 6Hz stimulation emerged as the most effective protocol for enhancing inhibitory control and cardiac interoception. By contrast, 2Hz stimulation increased impulsivity and reduced heart–brain connectivity by exerting suppressive carryover effects on subsequent 6Hz stimulation. Collectively, these results suggest that 6Hz stimulation is a candidate for future interventions targeting self-regulation and interoceptive awareness.

The stronger involvement of the 6Hz auditory stimulation may also be related to the recruitment of additional neurophysiological pathways, particularly those mediated by the vestibular system. Vestibular-evoked myogenic potentials (VEMPs) reflect vestibular afferent activation and are preferentially elicited using 6Hz tone bursts (Todd, Paillard et al. 2014, Jurado and Marquardt 2020). It is plausible that 6Hz Sonoception stimuli engaged vestibular pathways via this mechanism. Notably, the vestibular system maintains both structural and functional connections to the insular cortex, in particular at the level of the parieto-insular vestibular cortex (PIVC) (Kirsch, Keeser et al. 2016). In primates, the PIVC is a core node for vestibular processing (Lopez and Blanke 2011), and converging vestibular afferents from otolith organs and semicircular canals project to the retroinsular cortex, parietal operculum, and posterior insula (Lopez, Blanke et al. 2012).

Although preliminary, these converging lines of evidence suggest that both auditory and vestibular-insular pathways may contribute to the effects of 6Hz Sonoception. Future research is needed to delineate the relative contributions of these pathways and clarify the underlying mechanisms. Further investigations should also extend these findings to other insular-related domains, such as task-related interoceptive accuracy (Critchley, Wiens et al. 2004, Wang, Wu et al. 2019, Haruki and Ogawa 2021), pain perception (Lu, Yang et al. 2016, Labrakakis 2023), emotional awareness and regulation (Giuliani, Drabant et al. 2011, Gu, Hof et al. 2013, Li, Yang et al. 2021), decision-making (Rogers-Carter and Christianson 2019), and multisensory integration (Chen, Michels et al. 2015, Brunert and Rothermel 2020). Clinical applications should also be explored in populations with documented insular alterations, including major depression (Sliz and Hayley 2012, Pastrnak, Simkova et al. 2021, Hu, He et al. 2023), obsessive-compulsive disorder

(Nishida, Narumoto et al. 2011, Zhang, Xie et al. 2024), anxiety disorder (Paulus and Stein 2006), and addiction (Droutman, Read et al. 2015, Naqvi and Bechara 2015).

Conclusion

In a series of studies, we demonstrated that Sonoception auditory synthetic stimulation can either promote inhibitory control or enhance impulsivity, according to the frequency of the stimulation. Moreover, the synthetic stimulation was able to enhance HEPs activity, a proxy of heart-brain cortical processing, and activate the insular cortex in an fMRI resting state paradigm. Sonoception meets the demand for new methods in research (Garfinkel, Schulz et al. 2022) and may help us advance our understanding of the complex interplay between the processing of external and internal information, as well as design new methods and paradigms for both the healthy and clinical population. In line with this, it is crucial that future research investigates the underlying mechanisms of this non-invasive stimulation technique.

887 **Transparency and openness**

888 Following JARS (Kazak 2018), the manuscript reports how we determined our sample size, all
889 data exclusions if and when applied, and all measures in the study. Data, analysis code, and research
890 materials are available upon reasonable request directed at the corresponding author. The studies'
891 designs and analyses were not pre-registered.

892

893 **Acknowledgements**

894 M.T. was supported by the European Research Council Consolidator Grant (ERC-2016-CoG-
895 724537) under the FP7 for the INtheSELF project. For Study 3, D.D.L. was supported by
896 Experimental Psychological Society (EPS) Study visit Award for the project 'Effects of auditory
897 stimulation on affective Go/No-go task: an fMRI study".

898

899 **Authors contributions**

900 For Study 1: Conceptualization: D.D.L; Methodology: D.D.L., A.H., M.T.; Data collection:
901 D.D.L., G.F., V.V.; Data Analysis: D.D.L., G.F., V.V.; Writing - Original Draft Preparation,
902 D.D.L.; Writing - Review & Editing: V.V., G.R., M.T.; Supervision: G.R., M.T. For Study 2:
903 Conceptualization: D.D.L., A.Z.; Methodology: A.Z.; Data collection: A.Z.; Data Analysis: A.Z.;
904 Writing - Original Draft Preparation, D.D.L., A.Z.; Writing - Review & Editing: A.Z., D.D.L.,
905 V.V., M.C., F.F., G.R., M.T.; Supervision: M.C., F.F., G.R., M.T. For Study 3: Conceptualization:
906 D.D.L.; Methodology: A.H., M.T.; Data collection: A.H.; Data Analysis: A.H., F.F.; Writing -
907 Original Draft Preparation: A.H., F.F., D.D.L.; Writing - Review & Editing: D.D.L., V.V., M.C.,
908 F.F., G.R., M.T.; Supervision: M.C., F.F., G.R., M.T.

References

Ackermann, H. and A. Riecker (2004). "The contribution of the insula to motor aspects of speech production: a review and a hypothesis." Brain Lang **89**(2): 320-328.

Ackermann, H., A. Riecker, K. Mathiak, M. Erb, W. Grodd and D. Wildgruber (2001). "Rate-dependent activation of a prefrontal-insular-cerebellar network during passive listening to trains of click stimuli: an fMRI study." Neuroreport **12**(18): 4087-4092.

Al, E., F. Iliopoulos, N. Forschack, T. Nierhaus, M. Grund, P. Motyka, M. Gaebler, V. V. Nikulin and A. Villringer (2020). "Heart–brain interactions shape somatosensory perception and evoked potentials." **117**(19): 10575-10584.

Al, E., F. Iliopoulos, V. V. Nikulin and A. Villringer (2021). "Heartbeat and somatosensory perception." NeuroImage **238**: 118247.

Antonacci, Y., C. Barà, A. Zaccaro, F. Ferri, R. Pernice and L. Faes (2023). "Time-varying information measures: an adaptive estimation of information storage with application to brain-heart interactions." Front Netw Physiol **3**: 1242505.

Augustine, J. R. (1996). "Circuitry and functional aspects of the insular lobe in primates including humans." Brain research reviews **22**(3): 229-244.

Babo-Rebelo, M., A. Buot and C. Tallon-Baudry (2019). "Neural responses to heartbeats distinguish self from other during imagination." NeuroImage **191**: 10-20.

Babo-Rebelo, M., N. Wolpert, C. Adam, D. Hasboun and C. Tallon-Baudry (2016). "Is the cardiac monitoring function related to the self in both the default network and right anterior insula?" Philos Trans R Soc Lond B Biol Sci **371**(1708).

Bach, D. R., K. J. Friston and R. J. Dolan (2010). "Analytic measures for quantification of arousal from spontaneous skin conductance fluctuations." International Journal of Psychophysiology **76**(1): 52-55.

Bamiou, D. E., F. E. Musiek and L. M. Luxon (2003). "The insula (Island of Reil) and its role in auditory processing. Literature review." Brain Res Brain Res Rev **42**(2): 143-154.

Barà, C., A. Zaccaro, Y. Antonacci, M. Dalla Riva, A. Busacca, F. Ferri, L. Faes and R. Pernice (2023). "Local and global measures of information storage for the assessment of heartbeat-evoked cortical responses." Biomedical Signal Processing and Control **86**: 105315.

Bates, D., M. Mächler, B. Bolker and S. Walker (2015). "Fitting Linear Mixed-Effects Models Using lme4." Journal of Statistical Software **67**(1): 1 - 48.

Berger, J. I., H. Kawasaki, M. I. Banks, S. Kumar, M. A. Howard and K. V. Nourski (2025). "Human insula neurons respond to simple sounds during passive listening." bioRxiv: 2025.2003.2012.642819.

Blenkmann, A. O., S. Collavini, J. Lubell, A. Llorens, I. Funderud, J. Ivanovic, P. G. Larsson, T. R. Meling, T. Bekinschtein, S. Kochen, T. Endestad, R. T. Knight and A. K. Solbakk (2019). "Auditory deviance detection in the human insula: An intracranial EEG study." Cortex **121**: 189-200.

947 Brunert, D. and M. Rothermel (2020). "Cortical multisensory integration—a special role of the
948 agranular insular cortex?" Archiv-European Journal of Physiology **472**(6): 671-672.

949 Canales-Johnson, A., C. Silva, D. Huepe, Á. Rivera-Rei, V. Noreika, M. d. C. Garcia, W. Silva,
950 C. Ciraolo, E. Vaucheret, L. Sedeño, B. Couto, L. Kargieman, F. Baglivo, M. Sigman, S. Chennu,
951 A. Ibáñez, E. Rodríguez and T. A. Bekinschtein (2015). "Auditory Feedback Differentially
952 Modulates Behavioral and Neural Markers of Objective and Subjective Performance When
953 Tapping to Your Heartbeat." Cerebral Cortex **25**(11): 4490-4503.

954 Candia-Rivera, D., V. Catrambone and G. Valenza (2021). "The role of electroencephalography
955 electrical reference in the assessment of functional brain–heart interplay: From methodology to
956 user guidelines." Journal of Neuroscience Methods **360**: 109269.

957 Cauda, F., F. D'agata, K. Sacco, S. Duca, G. Geminiani and A. Vercelli (2011). "Functional
958 connectivity of the insula in the resting brain." Neuroimage **55**(1): 8-23.

959 Chen, T., L. Michels, K. Supekar, J. Kochalka, S. Ryali and V. Menon (2015). "Role of the
960 anterior insular cortex in integrative causal signaling during multisensory auditory–visual
961 attention." European Journal of Neuroscience **41**(2): 264-274.

962 Chouchou, F., F. Mauguière, O. Vallayer, H. Catenoix, J. Isnard, A. Montavont, J. Jung, V.
963 Pichot, S. Rheims and L. Mazzola (2019). "How the insula speaks to the heart: Cardiac responses
964 to insular stimulation in humans." Hum Brain Mapp **40**(9): 2611-2622.

965 Christison-Lagay, K. L., A. Khalaf, N. C. Freedman, C. Micek, S. I. Kronemer, M. M. Gusso, L.
966 Kim, S. Forman, J. Ding, M. Aksen, A. Abdel-Aty, H. Kwon, N. Markowitz, E. Yeagle, E.
967 Espinal, J. Herrero, S. Bickel, J. Young, A. Mehta, K. Wu, J. Gerrard, E. Damisah, D. Spencer
968 and H. Blumenfeld (2025). "The neural activity of auditory conscious perception." NeuroImage
969 **308**: 121041.

970 Citi, L., E. N. Brown and R. Barbieri (2012). "A Real-Time Automated Point-Process Method for
971 the Detection and Correction of Erroneous and Ectopic Heartbeats." IEEE Transactions on
972 Biomedical Engineering **59**(10): 2828-2837.

973 Coll, M. P., H. Hobson, G. Bird and J. Murphy (2021). "Systematic review and meta-analysis of
974 the relationship between the heartbeat-evoked potential and interoception." Neurosci Biobehav
975 Rev **122**: 190-200.

976 Cortese, M. D., M. Vatrano, P. Tonin, A. Cerasa and F. Riganello (2022). "Inhibitory Control and
977 Brain-Heart Interaction: An HRV-EEG Study." Brain Sci **12**(6).

978 Craig, A. D. (2002). "How do you feel? Interoception: the sense of the physiological condition of
979 the body." Nature reviews. Neuroscience **3**(8): 655-666.

980 Craig, A. D. (2003). "Interoception: the sense of the physiological condition of the body."
981 Current Opinion in Neurobiology **13**(4): 500-505.

982 Craig, A. D. (2009). "How do you feel--now? The anterior insula and human awareness." Nature
983 reviews neuroscience **10**(1).

984 Craig, A. D. (2010). "The sentient self." Brain Struct Funct **214**(5-6): 563-577.

985 Critchley, H. D., S. Wiens, P. Rotshtein, A. Öhman and R. J. Dolan (2004). "Neural systems
986 supporting interoceptive awareness." Nature neuroscience **7**(2): 189-195.

987 Dambacher, F., A. T. Sack, J. Lobbestael, A. Arntz, S. Brugman and T. Schuhmann (2015). "Out
988 of control: evidence for anterior insula involvement in motor impulsivity and reactive
989 aggression." Soc Cogn Affect Neurosci **10**(4): 508-516.

990 Delorme, A. and S. Makeig (2004). "EEGLAB: an open source toolbox for analysis of single-trial
991 EEG dynamics including independent component analysis." Journal of Neuroscience Methods
992 **134**(1): 9-21.

993 Droutman, V., S. J. Read and A. Bechara (2015). "Revisiting the role of the insula in addiction."
994 Trends in cognitive sciences **19**(7): 414-420.

995 Faul, F., E. Erdfelder, A. G. Lang and A. Buchner (2007). "G*Power 3: a flexible statistical
996 power analysis program for the social, behavioral, and biomedical sciences." Behav Res Methods
997 **39**(2): 175-191.

998 Frot, M., F. Mauguière and L. Garcia-Larrea (2022). "Insular dichotomy in the implicit detection
999 of emotions in human faces." Cerebral Cortex **32**(19): 4215-4228.

1000 García-Cordero, I., S. Esteves, E. P. Mikulan, E. Hesse, F. H. Baglivo, W. Silva, M. D. C. García,
1001 E. Vaucheret, C. Ciraolo, H. S. García, F. Adolfi, M. Pietto, E. Herrera, A. Legaz, F. Manes, A.
1002 M. García, M. Sigman, T. A. Bekinschtein, A. Ibáñez and L. Sedeño (2017). "Attention, in and
1003 Out: Scalp-Level and Intracranial EEG Correlates of Interoception and Exteroception." Front
1004 Neurosci **11**: 411.

1005 Garfinkel, S. N., A. Schulz and M. Tsakiris (2022). "Addressing the need for new interoceptive
1006 methods." Biological Psychology **170**: 108322.

1007 Ghahremani, A., A. Rastogi and S. Lam (2015). "The role of right anterior insula and salience
1008 processing in inhibitory control." J Neurosci **35**(8): 3291-3292.

1009 Giuliani, N. R., E. M. Drabant, R. Bhatnagar and J. J. Gross (2011). "Emotion regulation and
1010 brain plasticity: expressive suppression use predicts anterior insula volume." Neuroimage **58**(1):
1011 10-15.

1012 Gogolla, N. (2017). "The insular cortex." Current Biology **27**(12): R580-R586.

1013 Gogolla, N. (2017). "The insular cortex." Curr Biol **27**(12): R580-r586.

1014 Gu, X., P. R. Hof, K. J. Friston and J. Fan (2013). "Anterior insular cortex and emotional
1015 awareness." J Comp Neurol **521**(15): 3371-3388.

1016 Happer, J. P., L. C. Wagner, L. E. Beaton, B. Q. Rosen and K. Marinkovic (2021). "The “when”
1017 and “where” of the interplay between attentional capture and response inhibition during a
1018 Go/NoGo variant." NeuroImage **231**: 117837.

1019 Haruki, Y. and K. Ogawa (2021). "Role of anatomical insular subdivisions in interoception:
1020 Interoceptive attention and accuracy have dissociable substrates." European journal of
1021 neuroscience **53**(8): 2669-2680.

1022 Hassanpour, M. S., W. K. Simmons, J. S. Feinstein, Q. Luo, R. C. Lapidus, J. Bodurka, M. P.
1023 Paulus and S. S. Khalsa (2018). "The Insular Cortex Dynamically Maps Changes in
1024 Cardiorespiratory Interoception." Neuropsychopharmacology **43**(2): 426-434.

Herdener, M., C. Lehmann, F. Esposito, F. di Salle, A. Federspiel, D. R. Bach, K. Scheffler and E. Seifritz (2009). "Brain responses to auditory and visual stimulus offset: shared representations of temporal edges." Hum Brain Mapp **30**(3): 725-733.

Hu, L., H. He, N. Roberts, J. Chen, G. Yan, L. Pu, X. Song and C. Luo (2023). "Insular dysfunction of interoception in major depressive disorder: from the perspective of neuroimaging." Frontiers in Psychiatry **14**: 1273439.

Hung, Y., S. L. Gaillard, P. Yarmak and M. Arsalidou (2018). "Dissociations of cognitive inhibition, response inhibition, and emotional interference: Voxelwise ALE meta-analyses of fMRI studies." **39**(10): 4065-4082.

Hyvarinen, A. (1999). "Fast and robust fixed-point algorithms for independent component analysis." IEEE Transactions on Neural Networks **10**(3): 626-634.

Junghöfer, M., T. Elbert, D. M. Tucker and B. Rockstroh (2000). "Statistical control of artifacts in dense array EEG/MEG studies." **37**(4): 523-532.

Jurado, C. and T. Marquardt (2020). "On the Effectiveness of airborne infrasound in eliciting vestibular-evoked myogenic responses." **39**(1): 3-16.

Kato, Y., Y. Takei, S. Umeda, M. Mimura and M. Fukuda (2020). "Alterations of Heartbeat Evoked Magnetic Fields Induced by Sounds of Disgust." Front Psychiatry **11**: 683.

Kazak, A. E. (2018). "Journal article reporting standards."

Kern, M., A. Aertsen, A. Schulze-Bonhage and T. Ball (2013). "Heart cycle-related effects on event-related potentials, spectral power changes, and connectivity patterns in the human ECoG." NeuroImage **81**: 178-190.

Kirsch, V., D. Keeser, T. Hergenroeder, O. Erat, B. Ertl-Wagner, T. Brandt and M. Dieterich (2016). "Structural and functional connectivity mapping of the vestibular circuitry from human brainstem to cortex." Brain Structure and Function **221**(3): 1291-1308.

Labrakakis, C. (2023). "The Role of the Insular Cortex in Pain." Int J Mol Sci **24**(6).

Labrakakis, C. (2023). "The role of the insular cortex in pain." International Journal of Molecular Sciences **24**(6): 5736.

Lenth, R., H. Singmann, J. Love, P. Buerkner and M. Herve (2019). Package 'emmeans'.

Li, W., P. Yang, R. K. Ngetich, J. Zhang, Z. Jin and L. Li (2021). "Differential involvement of frontoparietal network and insula cortex in emotion regulation." Neuropsychologia **161**: 107991.

Lopez-Calderon, J. and S. J. Luck (2014). "ERPLAB: an open-source toolbox for the analysis of event-related potentials." **8**.

Lopez, C. and O. Blanke (2011). "The thalamocortical vestibular system in animals and humans." Brain Research Reviews **67**(1): 119-146.

Lopez, C., O. Blanke and F. W. Mast (2012). "The human vestibular cortex revealed by coordinate-based activation likelihood estimation meta-analysis." Neuroscience **212**: 159-179.

Lu, C., T. Yang, H. Zhao, M. Zhang, F. Meng, H. Fu, Y. Xie and H. Xu (2016). "Insular cortex is critical for the perception, modulation, and chronification of pain." Neuroscience bulletin **32**(2): 191-201.

Lüdecke, D., M. S. Ben-Shachar, I. Patil, P. Waggoner and D. J. J. o. O. S. S. Makowski (2021). "performance: An R package for assessment, comparison and testing of statistical models." **6**(60).

Luft, C. D. B. and J. Bhattacharya (2015). "Aroused with heart: Modulation of heartbeat evoked potential by arousal induction and its oscillatory correlates." Scientific Reports **5**(1): 15717.

Mai, S., C. K. Wong, E. Georgiou and O. Pollatos (2018). "Interoception is associated with heartbeat-evoked brain potentials (HEPs) in adolescents." Biological Psychology **137**: 24-33.

Mazzola, V., G. Arciero, L. Fazio, T. Lanciano, B. Gelao, T. Popolizio, P. Vuilleumier, G. Bondolfi and A. Bertolino (2016). "What Impact does An Angry Context have Upon Us? The Effect of Anger on Functional Connectivity of the Right Insula and Superior Temporal Gyri." Front Behav Neurosci **10**: 109.

Menon, V., N. E. Adleman, C. D. White, G. H. Glover and A. L. Reiss (2001). "Error-related brain activation during a Go/NoGo response inhibition task." Hum Brain Mapp **12**(3): 131-143.

Mesulam, M. M. and E. J. Mufson (1982). "Insula of the old world monkey. III: Efferent cortical output and comments on function." Journal of Comparative Neurology **212**(1): 38-52.

Namkung, H., S. H. Kim and A. Sawa (2017). "The Insula: An Underestimated Brain Area in Clinical Neuroscience, Psychiatry, and Neurology." Trends Neurosci **40**(4): 200-207.

Naqvi, N. H. and A. Bechara (2015). "The Insula: A Critical Neural Substrate for Drug Seeking under Conflict and Risk." The Wiley Handbook on the Cognitive Neuroscience of Addiction: 128-150.

Nishida, S., J. Narumoto, Y. Sakai, T. Matsuoka, T. Nakamae, K. Yamada, T. Nishimura and K. Fukui (2011). "Anterior insular volume is larger in patients with obsessive–compulsive disorder." Progress in Neuro-Psychopharmacology

Biological psychiatry. Cognitive neuroscience and neuroimaging **35**(4): 997-1001.

Nourski, K. V., M. Steinschneider, A. E. Rhone, C. K. Kovach, H. Kawasaki and M. A. Howard (2022). "Gamma activation and alpha suppression within human auditory cortex during a speech classification task." Journal of Neuroscience **42**(25): 5034-5046.

Oh, A., E. G. Duerden and E. W. Pang (2014). "The role of the insula in speech and language processing." Brain Lang **135**: 96-103.

Pan, J. and W. J. Tompkins (1985). "A real-time QRS detection algorithm." IEEE Trans Biomed Eng **32**(3): 230-236.

Papagno, C., A. Pisoni, G. Mattavelli, A. Casarotti, A. Comi, F. Fumagalli, M. Vernice, E. Fava, M. Riva and L. Bello (2016). "Specific disgust processing in the left insula: New evidence from direct electrical stimulation." Neuropsychologia **84**: 29-35.

Park, H. D., F. Bernasconi, J. Bello-Ruiz, C. Pfeiffer, R. Salomon and O. Blanke (2016). "Transient Modulations of Neural Responses to Heartbeats Covary with Bodily Self-Consciousness." J Neurosci **36**(32): 8453-8460.

Park, H. D., F. Bernasconi, R. Salomon, C. Tallon-Baudry, L. Spinelli, M. Seeck, K. Schaller and O. Blanke (2018). "Neural Sources and Underlying Mechanisms of Neural Responses to

Heartbeats, and their Role in Bodily Self-consciousness: An Intracranial EEG Study." Cereb Cortex **28**(7): 2351-2364.

Park, H. D. and O. Blanke (2019). "Heartbeat-evoked cortical responses: Underlying mechanisms, functional roles, and methodological considerations." Neuroimage **197**: 502-511.

Pastrnak, M., E. Simkova and T. Novak (2021). "Insula activity in resting-state differentiates bipolar from unipolar depression: a systematic review and meta-analysis." Scientific reports **11**(1): 16930.

Paulus, M. P. and M. B. Stein (2006). "An insular view of anxiety." Biological psychiatry **60**(4): 383-387.

Perakakis, P. (2019). "HEPLAB: a Matlab graphical interface for the preprocessing of the heartbeatevoked potential (Version v1. 0.0)." Zenodo **2649943**.

Petzschner, F. H., L. A. Weber, K. V. Wellstein, G. Paolini, C. T. Do and K. E. Stephan (2019). "Focus of attention modulates the heartbeat evoked potential." NeuroImage **186**: 595-606.

Piarulli, A., A. Zaccaro, M. Laurino, D. Menicucci, A. De Vito, L. Bruschini, S. Berrettini, M. Bergamasco, S. Laureys and A. Gemignani (2018). "Ultra-slow mechanical stimulation of olfactory epithelium modulates consciousness by slowing cerebral rhythms in humans." Scientific Reports **8**(1): 6581.

Protas, M. (2018). Role of the insula in visual and auditory perception. Island of Reil (Insula) in the human brain: Anatomical, functional, clinical and surgical aspects, Springer**:** 151-156.

Remedios, R., N. K. Logothetis and C. Kayser (2009). "An auditory region in the primate insular cortex responding preferentially to vocal communication sounds." Neurosci **29**(4): 1034-1045.

Renier, L. A., I. Anurova, A. G. De Volder, S. Carlson, J. VanMeter and J. P. Rauschecker (2009). "Multisensory integration of sounds and vibrotactile stimuli in processing streams for "what" and "where"." Journal of Neuroscience **29**(35): 10950-10960.

Riva, G., S. Serino, D. Di Lernia, E. F. Pavone and A. Dakanalis (2017). "Embodied medicine: Mens sana in corpore virtuale sano." Frontiers in Human Neuroscience **11**.

Rogers-Carter, M. M. and J. P. Christianson (2019). "An insular view of the social decision-making network." Neuroscience

Biobehavioral Reviews **103**: 119-132.

Salomon, R., R. Ronchi, J. Dönz, J. Bello-Ruiz, B. Herbelin, N. Faivre, K. Schaller and O. Blanke (2018). "Insula mediates heartbeat related effects on visual consciousness." Cortex **101**: 87-95.

Seok, J. W. and C. Cheong (2019). "Dynamic Causal Modeling of Effective Connectivity During Anger Experience in Healthy Young Men: 7T Magnetic Resonance Imaging Study." Adv Cogn Psychol **15**(1): 52-62.

Seth, A. K. (2013). "Interoceptive inference, emotion, and the embodied self." Trends Cogn Sci **17**(11): 565-573.

Seth, A. K. and K. J. Friston (2016). "Active interoceptive inference and the emotional brain." Philos Trans R Soc Lond B Biol Sci **371**(1708).

1142 Singer, T., H. D. Critchley and K. Preuschoff (2009). "A common role of insula in feelings,
1143 empathy and uncertainty." Trends Cogn Sci **13**(8): 334-340.

1144 Sliz, D. and S. Hayley (2012). "Major depressive disorder and alterations in insular cortical
1145 activity: a review of current functional magnetic imaging research." Frontiers in human
1146 neuroscience **6**: 323.

1147 Takemoto, M., K. Hasegawa, M. Nishimura and W. J. Song (2014). "The insular auditory field
1148 receives input from the lemniscal subdivision of the auditory thalamus in mice." Journal of
1149 Comparative Neurology **522**(6): 1373-1389.

1150 Tarvainen, M. P., J.-P. Niskanen, J. A. Lipponen, P. O. Ranta-aho and P. A. Karjalainen (2014).
1151 "Kubios HRV – Heart rate variability analysis software." Computer Methods and Programs in
1152 Biomedicine **113**(1): 210-220.

1153 Todd, N. P., A. C. Paillard, K. Kluk, E. Whittle and J. G. Colebatch (2014). "Source analysis of
1154 short and long latency vestibular-evoked potentials (VsEPs) produced by left vs. right ear air-
1155 conducted 500 Hz tone pips." Hear Res **312**(100): 91-102.

1156 Tottenham, N., T. Hare and B. J. Casey (2011). "Behavioral Assessment of Emotion
1157 Discrimination, Emotion Regulation, and Cognitive Control in Childhood, Adolescence, and
1158 Adulthood." Frontiers in Psychology **2**(39).

1159 Villena-González, M., V. López and E. Rodríguez (2016). "Data of ERPs and spectral alpha
1160 power when attention is engaged on visual or verbal/auditory imagery." Data in Brief **7**: 882-888.

1161 Vytal, K. and S. Hamann (2010). "Neuroimaging support for discrete neural correlates of basic
1162 emotions: a voxel-based meta-analysis." J Cogn Neurosci **22**(12): 2864-2885.

1163 Wang, X., Q. Wu, L. Egan, X. Gu, P. Liu, H. Gu, Y. Yang, J. Luo, Y. Wu and Z. Gao (2019).
1164 "Anterior insular cortex plays a critical role in interoceptive attention." elife **8**: e42265.

1165 Wicker, B., C. Keysers, J. Plailly, J. P. Royet, V. Gallese and G. Rizzolatti (2003). "Both of us
1166 disgusted in My insula: the common neural basis of seeing and feeling disgust." Neuron **40**(3):
1167 655-664.

1168 Wright, P., G. He, N. A. Shapira, W. K. Goodman and Y. Liu (2004). "Disgust and the insula:
1169 fMRI responses to pictures of mutilation and contamination." Neuroreport **15**(15): 2347-2351.

1170 Zaccaro, A., F. della Penna, E. Mussini, E. Parrotta, M. G. Perrucci, M. Costantini and F. Ferri
1171 (2024). "Attention to cardiac sensations enhances the heartbeat-evoked potential during
1172 exhalation." iScience **27**(4): 109586.

1173 Zaccaro, A., M. G. Perrucci, E. Parrotta, M. Costantini and F. Ferri (2022). "Brain-heart
1174 interactions are modulated across the respiratory cycle via interoceptive attention." NeuroImage
1175 **262**: 119548.

1176 Zaccaro, A., A. Piarulli, L. Melosini, D. Menicucci and A. Gemignani (2022). "Neural Correlates
1177 of Non-ordinary States of Consciousness in Pranayama Practitioners: The Role of Slow Nasal
1178 Breathing." **16**.

1179 Zhang, R., H. Deng and X. Xiao (2024). "The Insular Cortex: An Interface Between Sensation,
1180 Emotion and Cognition." Neuroscience Bulletin **40**(11): 1763-1773.

Zhang, X., M. Xie, W. Li, Z. Xu, Z. Wang, W. Jiang, Y. Wu and N. Liu (2024). "Abnormalities of structural covariance of insular subregions in drug-naïve OCD patients." Cerebral Cortex **34**(1): bhad469.

Zhang, Y., W. Zhou, J. Huang, B. Hong and X. Wang (2022). "Neural correlates of perceived emotions in human insula and amygdala for auditory emotion recognition." Neuroimage Clin **260**: 119502.

Zhang, Y., W. Zhou, S. Wang, Q. Zhou, H. Wang, B. Zhang, J. Huang, B. Hong and X. Wang (2019). "The Roles of Subdivisions of Human Insula in Emotion Perception and Auditory Processing." Cerebral Cortex **29**(2): 517-528.